AD-A021 142

CHARACTERIZATION OF BIRD IMPACTS ON A RIGID PLATE:
PART 1

John P. Barber, et al

Dayton University

Prepared for:

Air Force Flight Dynamics Laboratory

January 1975

063161

AFFDL-TR-75-5

ADA021142

CHARACTERIZATION OF BIRD IMPACTS ON A RIGID PLATE: PART 1

DR. JOHN P. BARBER
HENRY R. TAYLOR
UNIVERSITY OF DAYTON RESEARCH INSTITUTE

JAMES S. WILBECK
AIR FORCE MATERIALS LABORATORY

TECHNICAL REPORT AFFDL-TR-75-5

JANUARY 1975

Approved for public release; distribution unlimited.

AIR FORCE FLIGHT DYNAMICS LABORATORY
AIR FORCE SYSTEMS COMMAND
WRIGHT-PATTERSON AIR FORCE BASE, OHIO 45433

"This report has been reviewed and cleared
for open publication and/or public release by
the appropriate Office of Information (OI) in
accordance with AFR 190-170 and DODD 5230.9.
There is no objection to unlimited distribution of
this report to the public at large or by DDC to the
National Technical Information Service (NTIS)."

"This technical report has been reviewed and
is approved for publication."

RICHARD L. PETERSON, Project Engineer
Improved Windshield Protection ADPO
Vehicle Equipment Division
Air Force Flight Dynamics Laboratory

FOR THE COMMANDER

ROBERT E. WITTMAN, Program Manager
Improved Windshield Protection ADPO
Vehicle Equipment Division
Air Force Flight Dynamics Laboratory

ii

REPORT DOCUMENTATION PAGE		READ INSTRUCTIONS BEFORE COMPLETING FORM
1. REPORT NUMBER AFFDL-TR-75-5	2. GOVT ACCESSION NO.	3. RECIPIENT'S CATALOG NUMBER
4. TITLE (and Subtitle) CHARACTERIZATION OF BIRD IMPACTS ON A RIGID PLATE: PART 1		5. TYPE OF REPORT & PERIOD COVERED Technical Report 1 Jan 74 - 30 Nov 74
		6. PERFORMING ORG. REPORT NUMBER
7. AUTHOR(s) Dr. John P. Barber Henry R. Taylor James S. Wilbeck		8. CONTRACT OR GRANT NUMBER(s) F 33615-73-C-5027
9. PERFORMING ORGANIZATION NAME AND ADDRESS University of Dayton 300 College Park Ave. Dayton, Ohio 45469		10. PROGRAM ELEMENT, PROJECT, TASK AREA & WORK UNIT NUMBERS Project No. 7351 Task No. 735106 W. U. No. 73510689
11. CONTROLLING OFFICE NAME AND ADDRESS Air Force Flight Dynamics Lab Air Force Materials Lab Wright Patterson Air Force Base, Ohio		12. REPORT DATE January, 1975
		13. NUMBER OF PAGES
14. MONITORING AGENCY NAME & ADDRESS(if different from Controlling Office)		15. SECURITY CLASS. (of this report) UNCLASSIFIED
		15a. DECLASSIFICATION/DOWNGRADING SCHEDULE

16. DISTRIBUTION STATEMENT (of this Report)

Approved for public release; distribution unlimited

17. DISTRIBUTION STATEMENT (of the abstract entered in Block 20, if different from Report)

18. SUPPLEMENTARY NOTES

19. KEY WORDS (Continue on reverse side if necessary and identify by block number)

Bird Impacts, Impulsive Loading, Pressure Transducers

20. ABSTRACT (Continue on reverse side if necessary and identify by block number)

Techniques for launching small birds at up to 350 m/s have been developed. The birds are mounted in polyethylene sabots to provide support and confinement during acceleration. A satisfactory method of sabot stripping has also been developed. X-radiography and photography were used to verify bird orientation and integrity prior to impact.

Birds launched at up to 350 m/s were impacted into a rigid flat target and the pressures generated at impact were measured at the center of impact,

DD FORM 1473 EDITION OF 1 NOV 65 IS OBSOLETE   i

1. 27 cm, 2. 54 cm and 3. 81 cm off center. Peak pressures as measured from oscillograph records of pressure time were determined as well as the variation of peak pressure with velocity, radial distance from center of impact and bird size. Impulse intensity ($\int Pdt$) was also measured and its variation with velocity determined.

Peak pressure was found to vary approximately as velocity squared and was independent of bird size. This suggests that the bird behaves as a fluid during impact.

FOREWORD

The program described in this report was carried out by
the University of Dayton at the Air Force Materials Laboratories,
Wright Patterson Air Force Base, Dayton, Ohio under contract
F33615-73-C-5027.

The work was conducted during the period January, 1974, to
November, 1974, and was co-monitored by Mr. Richard L. Peterson
of the Air Force Flight Dynamics Laboratory and Dr. Alan K. Hopkins
of the Air Force Materials Laboratory.

This report was submitted by the authors in January, 1975, for
publication as an AFFDL Technical Report.

TABLE OF CONTENTS

Preceding page blank

LIST OF ILLUSTRATIONS

Preceding page blank

LIST OF ILLUSTRATIONS (CONTD)

LIST OF TABLES

SELECTED CONVERSION FACTORS

Velocity:

1 meter/second (m/s) = 3.281 feet/second (ft/s)

Pressure:

10^6 newton/meter^2 (MN/m^2) = 145 pounds/inch^2 (psi)

Impulse Intensity:

10^3 newton-seconds/meter^2 (kNs/m^2) = .145 pound-seconds/inch^2 (psi-s)

Preceding page blank

SECTION 1

INTRODUCTION AND SUMMARY

Aircraft may be damaged or even destroyed by inflight impacts
with birds. Windshields and jet engine fan blades are particularly
vulnerable to damage by bird impacts.

The purpose of this study has been to experimentally determine the
pressure-time variations generated by small birds impacting a flat
rigid plate, in an effort to characterize the loading of real aircraft
components by bird impacts. Pressure data for two masses of birds
(approximately 70g and 125g), at velocities from 60 to 350 m/s,
were obtained by recording the output of pressure sensors on the
target plate located on trajectory axis and at distances of 1.27cm, 2.54cm,
and 3.81cm off trajectory axis.

The overall objectives of the program are:

i)   To characterize the loading behavior of birds at impact.
The ultimate characterization is regarded as a simple bird model
reducible to a simple mathematical model. A second, less satisfactory,
characterization consists simply of graphs describing pressure-time
variations as functions of velocity, radii from center of impact, and
bird size.

ii)   To characterize the response of real aircraft components
to the impact of birds. The response of sample components must be
quantified experimentally and related to the previously determined impact
loading of the component. Again, a simple model and associated
mathematical description are desired, but more sophisticated and
indepth computer analysis may be necessary.

iii)   To develop design methods and criteria. The successful
characterization of the impact of birds and subsequent response of

aircraft components will enable a more logical approach to the design
and test of FOD resistant aircraft components, thereby reducing the
cost and delay of developing and verifying such components.

A satisfactory technique for launching small birds at velocities
up to 350 m/s was developed. The birds were mounted in a polyethylene
sabot which provided confinement during acceleration. The sabot
was stripped from the bird and stopped at the muzzle by the cutting
and deformation of the sabot. The photographic records indicated
that bird integrity and desired orientation were maintained until
impact. The x-radiographs further indicated that there was
negligible internal damage to the bird during launch and sabot
deparation. Satisfactory separation of the sabot was obtained and
the sabot was contained at the muzzle to prevent any interference with
the bird before or during impact.

A double laser beam technique was used to obtain reliable bird
velocity measurements accurate to an estimated $\pm 1\%$. The technique
proved to be relatively insensitive to debris, such as detached feathers,
and considerable confidence can be placed in the velocity measurements.

Proven photographic techniques were employed (x-rays, flashed light
and cine) to produce corroborative data on bird integrity and orientation
before impact and permitted the direct observation of debris
distribution and velocity during impact.

A technique to measure the pressure on a rigid plate during impact
was developed. High amplitude, high frequency pressure
transducers were flush mounted in the plate and the outputs recorded
on an oscilloscope. A number of transducers were arranged on the plate
to provide a measure of the temporal and radial distribution of
pressure during impact. The high impact loads failed a number
of transducers in which impedance matching circuits were physically
located on the transducer. Another type of transducer in which the impedance
matching device was physically separated from the transducer
survived in excess of 80 impacts without failure. (Appendix D.)

2

This report includes measured impact velocities, x-radiographs and photographs showing bird condition and orientation for selected tests, and the pressure-time traces for each sensor for a selection of shots. Curves displaying the variation of peak pressure both as a function of velocity at various measuring stations and as a function of distance from the contact point for selected velocities are included.

SECTION 2
EXPERIMENTAL TECHNIQUES

2.1 LAUNCH TECHNIQUES AND REQUIREMENTS

The experiments required that two sizes of birds (chickens of approximately 70 g and 125 g) be launched intact at velocities ranging from 60 m/s to 350 m/s. Listed below are some of the pertinent launcher design considerations and constraints:

i) Overall range length limited to six meters.

ii) The projectile must be powder driven because of the large volume of gas required.

iii) Birds must be confined by saboting during acceleration because of their soft bodies.

iv) Acceleration must be kept sufficiently low to prevent destruction of the bird.

v) The bird must separate freely from the sabot.

vi) The sabot must be stopped in the launch tube or diverted from the bird trajectory to prevent the sabot from impacting the target.

vii) Acceleration must be removed from the bird for a sufficient period to permit the bird to "relax" before impact.

2.2 RANGE DESCRIPTION

The range facility consisted of a 8.90 cm bore powder driven gun, a blast tank and a target tank. The launch tube selected for this series of experiments was a 8.90 cm i/d, 11.43 cm o/d, 4.27 m length of seamless steel tubing. The ends of the tube were threaded to accept a breech block at the breech end and a sabot stopper at the muzzle. Four longitudinal slits 46 cm long, 0.318 cm wide, terminating 36 cm from the muzzle, were machined in the tube to vent the powder gas and permit the sabot to begin deceleration before striking the sabot stopper.

The breech block incorporated a soft launch buffer technique developed by the University of Dayton Research Institute (UDRI) during a previous bird launch feasibility study. Briefly, the buffer system consisted of a chamber in the breech block into which the powder gas expanded. The output port of the chamber was necked down to restrict gas flow into the gun. The objective of the breech design was to generate a low but constant acceleration pressure behind the projectile until the pressure was relieved by the longitudinal slits at the muzzle.

The launch tube was secured to a 36 cm x 51 cm "I" beam by three modified pipe vises. The launch tube was passed through the blast tank, where the powder gas was vented by the longitudinal slits previously mentioned, and extended into a 0.6 m cubic target tank. The target, a 15.25 cm diameter 5.1 cm thick steel disk, was mounted on the target tank wall approximately 36 cm from the gun muzzle.

The entire range was evacuated to an air pressure of 5 torr to maintain repeatable bird orientation at impact. A photograph of the overall range facility is shown in Figure 1.

2.3 SABOT AND SABOT SEPARATION

The development of a sabot that could be stopped in the launch tube with no detrimental effect on the bird involved a considerable search for an appropriate design and material.

The first approach was to use a Lexan sabot with sufficient wall thickness to withstand the impact forces generated when striking a sabot stripping stopper plate. This sabot worked reliably at velocities below 100 m/s, but at higher velocities the walls and end of the sabot were cracked and parts of the sabot continued down stream.

The mode of failure of the Lexan suggested that a more pliable material was required. Nylon and low density polyethylene were tested, but at velocities above 150 m/s the walls collapsed inward, trapping the bird before separation from the sabot was completed.

From the results of these tests it was concluded that a strong, pliable material was required and that the peak deceleration must be

Figure 1. Overall view of bird range facility.

reduced by means of a shock absorbing pad attached to the sabot stopper plate and/or by dissipating energy in the sabot during the deceleration. High density polyethylene was selected for its strength and pliability and a combination of both shock absorption and energy dissipation was obtained by cutting and deforming the sabot during deceleration while taking care not to distort the sabot pocket as demonstrated in Figure 2.

Figure 2. Typical sabots; after stopping (left), before launch (right).

A 1.27 cm thick hard rubber ring attached to the sabot stopper plate acted as a pad for the sabot wall to strike. A conical steel spreader ring with an interior diameter 0.65 cm greater than the diameter of the sabot pocket was attached to the stopper plate as shown in Figure 3. The spreader ring cut into the wall of the sabot forcing most of the wall to spread outward and into the stopper plate. Only the outer portion of the sabot wall was deformed and the pocket remains intact.
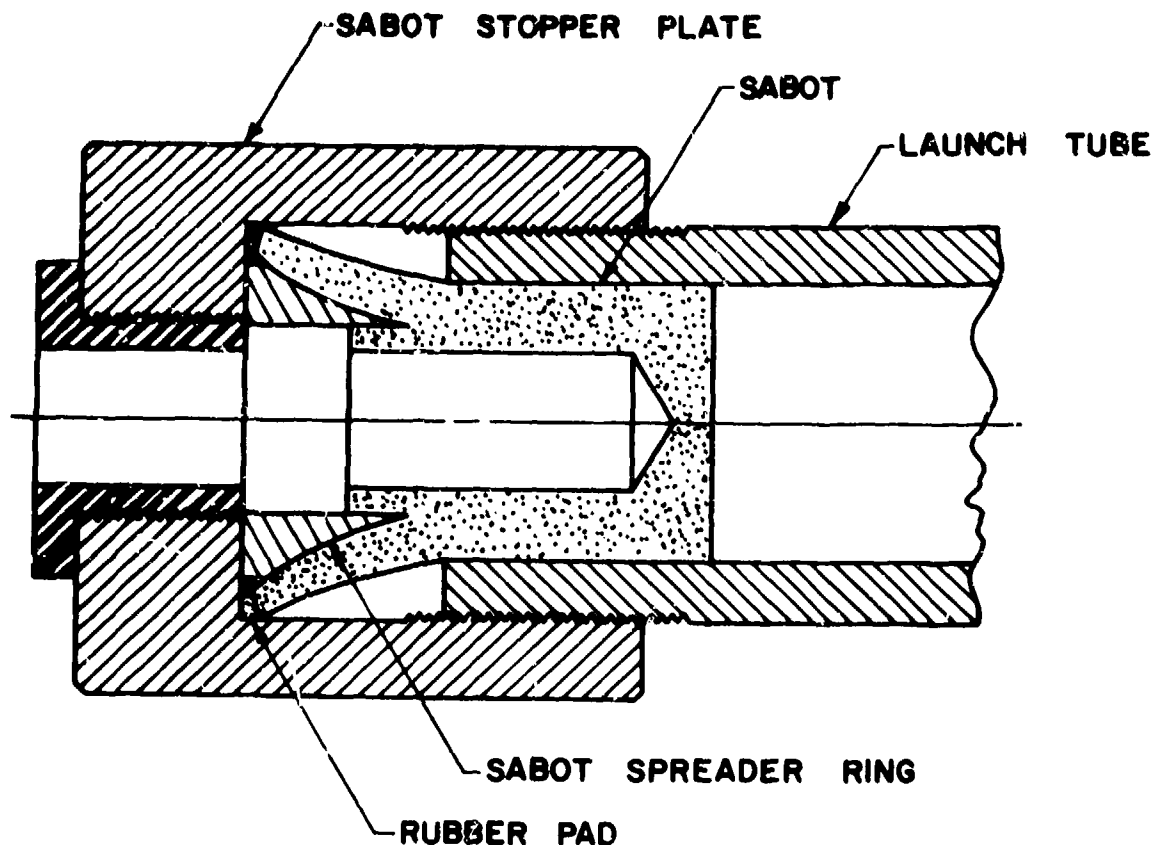
Figure 3. Sabot stopper.

Birds weighing 60 to 150 g were launched intact and properly oriented (i. e. axial) at velocities from 30 to 350 m/s. High speed x-radiographs and photographs indicated that bird integrity was maintained to velocities exceeding 300 m/s and orientation was satisfactory. (See Section 2. 4. 2.)

Satisfactory sabot separation was achieved and there were no secondary impacts of sabot material. The bird was released without any apparent damage or disruption to its attitude or flight path as evidenced by the x-radiographs and photographs. (See Section 2. 4. 2.)

A total of 47 shots were required to perfect the sabot design and generate a powder loading curve for the gun.

2.4 INSTRUMENTATION

2.4.1 Velocity Measurement

Velocity was calculated from the time of flight, as measured by a digital time interval counter, between the interruption of two pairs of laser beams arranged across the trajectory. Two laser beams were aligned at each station to form a triangular plane perpendicular to the projectile trajectory; the beams converging at the element of a photomultiplier tube. Because the beams were independent, they both had to be interrupted simultaneously to produce a signal of sufficient amplitude to overcome the bias on a built-in pulse amplifier and to generate a signal. The use of two lasers at each velocity station was necessary to assure that the velocity of the main body of the bird was measured and not the velocity of loose feathers or debirs. Photographs and x-radiographs verified the reliability of this trigger system.

The time of flight was typically of the order of 1 ms and was measured to 0.1 μs. It was estimated that the distance between stations was know to about 1% and, therefore, the measured velocity was accurate to about 1%.

2.4.2 Photography and X-radiography

Each bird launched was x-rayed and photographed immediately prior to impact to verify that it was properly oriented and intact. In addition, cine photographs of birds during impact were obtained to aid in the description and understanding of the bird breakup.

A 180 KV flash x-ray* unit with the head aimed vertically down and perpendicular to trajectory was employed. A 18 cm x 36 cm x-ray cassette was placed lengthwise along and 5 cm under the bird trajectory as shown in Figure 4.

The x-ray and light sources were triggered from the output of the first interrupted laser beam velocity measuring station described in Section 2.4.1.

* Field Emission Corporation Model No. 2722.

9
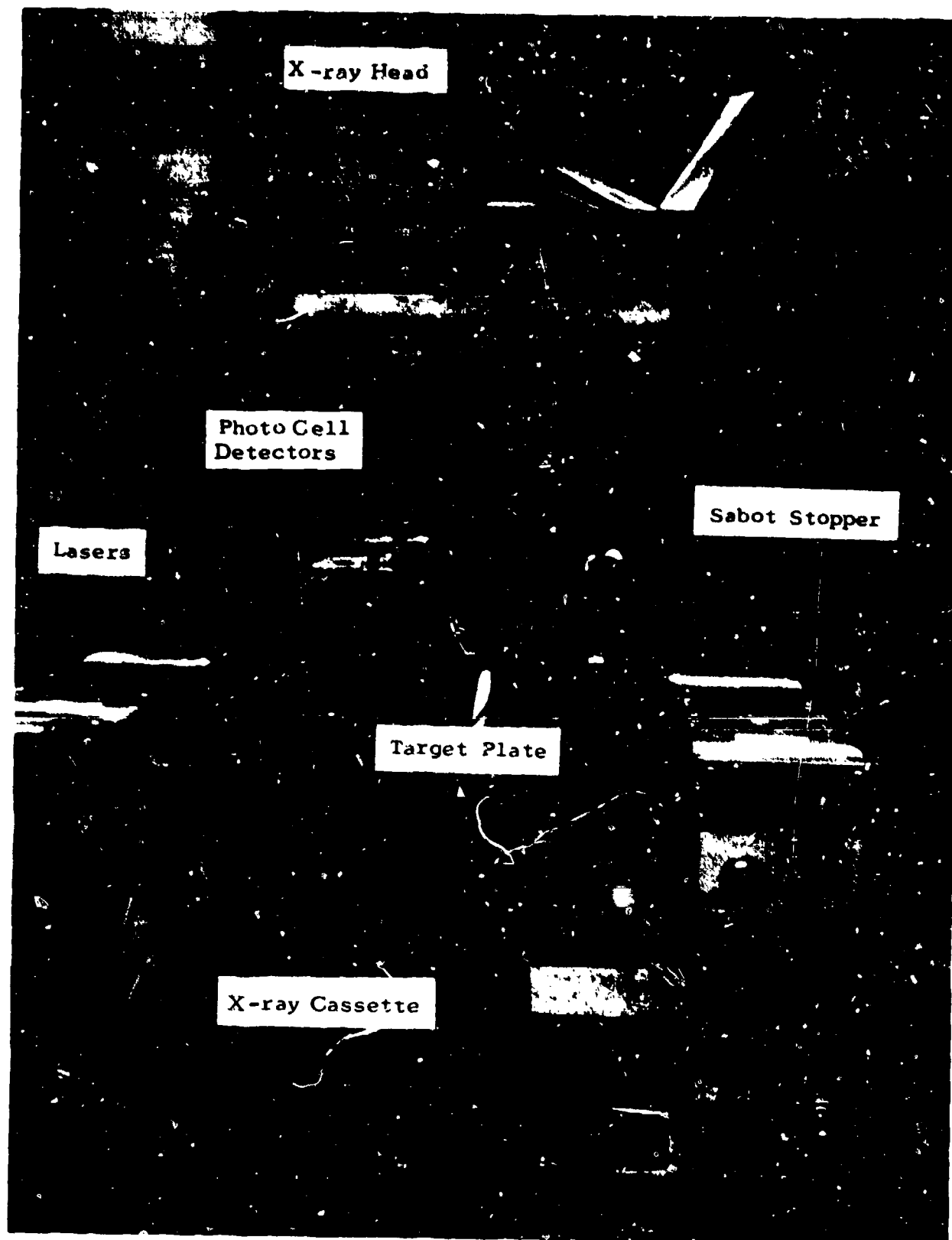
Figure 4. Target tank assembly.

Two typical x-radiographs are shown in Figure 5, one at
low velocity (Figure 5a) and one at high velocity (Figure 5b). Similar
x-radiographs were obtained for almost all shots in this series and
a selection of them is included in Appendix A.

The x-radiographs indicated that the bird was intact and
properly oriented prior to impact. All birds were launched tail
leading and impacted the plate in that orientation. Apparently, there
was no breaking or crushing of bones during launching for muzzle
velocities of up to 350 m/s.

A xenon flash tube light source and 10 cm x 12.5 cm camera
were used to obtain photographs of the bird prior to impact to verify the
x-radiographic results. Two typical photographs are shown in Figure 6,
one at low velocity (Figure 6a) and one at high velocity (Figure 6b).
Similar photographs were obtained for most of the shots in this series
and a selection of these is included in Appendix B.

These photograph, confirmed the results of the x-radiographs;
that is, the birds were intact and properly oriented (axial, tail first) at
impact. The shape of the bird prior to impact appeared to be approx-
imately cylindrical and there was some separation and clouding of the
feathers above 200 m/s.

A full framing 16 mm Fastax camera at a framing rate of 7500
frames per second was used to record the impact process in order to
observe bird breakup and debris distribution during and after impact. A
typical sequence is shown in Figure 7 and other selected sequences at
various angles of observation are collected in Appendix C.

The cine photographs of Figure 7 verified the observed good
axial symmetry in the preimpact photographs and indicated a high degree
of axial symmetry throughout the impact process. From this and similar
series of photographs shown in Appendix C the following observations
were made:

        i)   The angle with respect to the plane of the target
at which the debris exits from the impact was low; that is, there was
practically no rebound of the bird debris. This implied that the impulse

Shot no. 4970; velocity 62.8 m/s
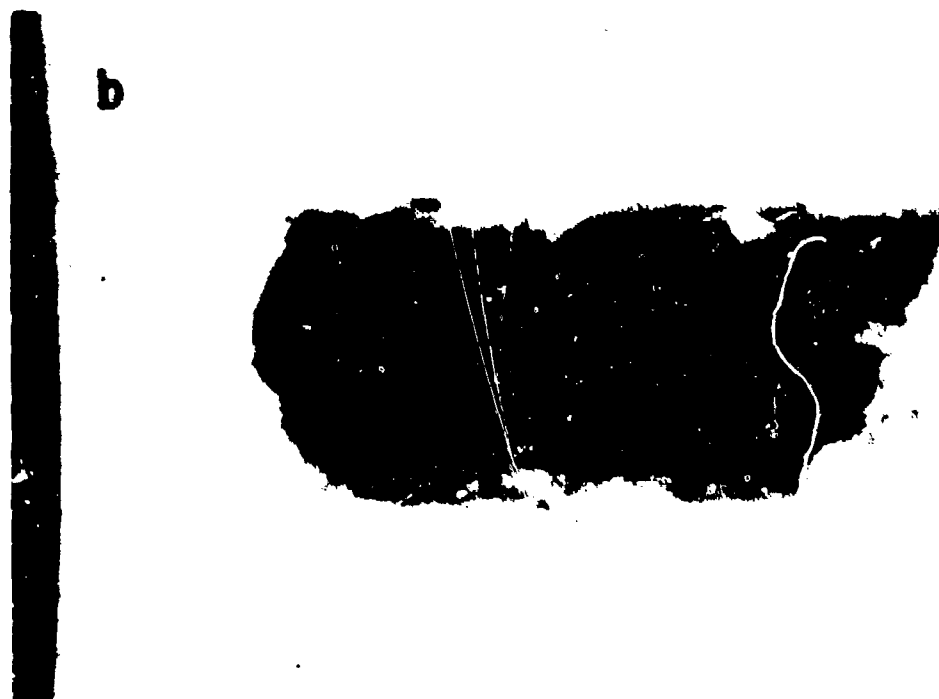
Shot no. 4962; velocity 253 m/s

Figure 5.   X-radiographs of launched birds.

Shot no. 4970; velocity 62. 8 m/s

Shot no. 4962; velocity 253 m/e

Figure 6. Photographs of launched birds.
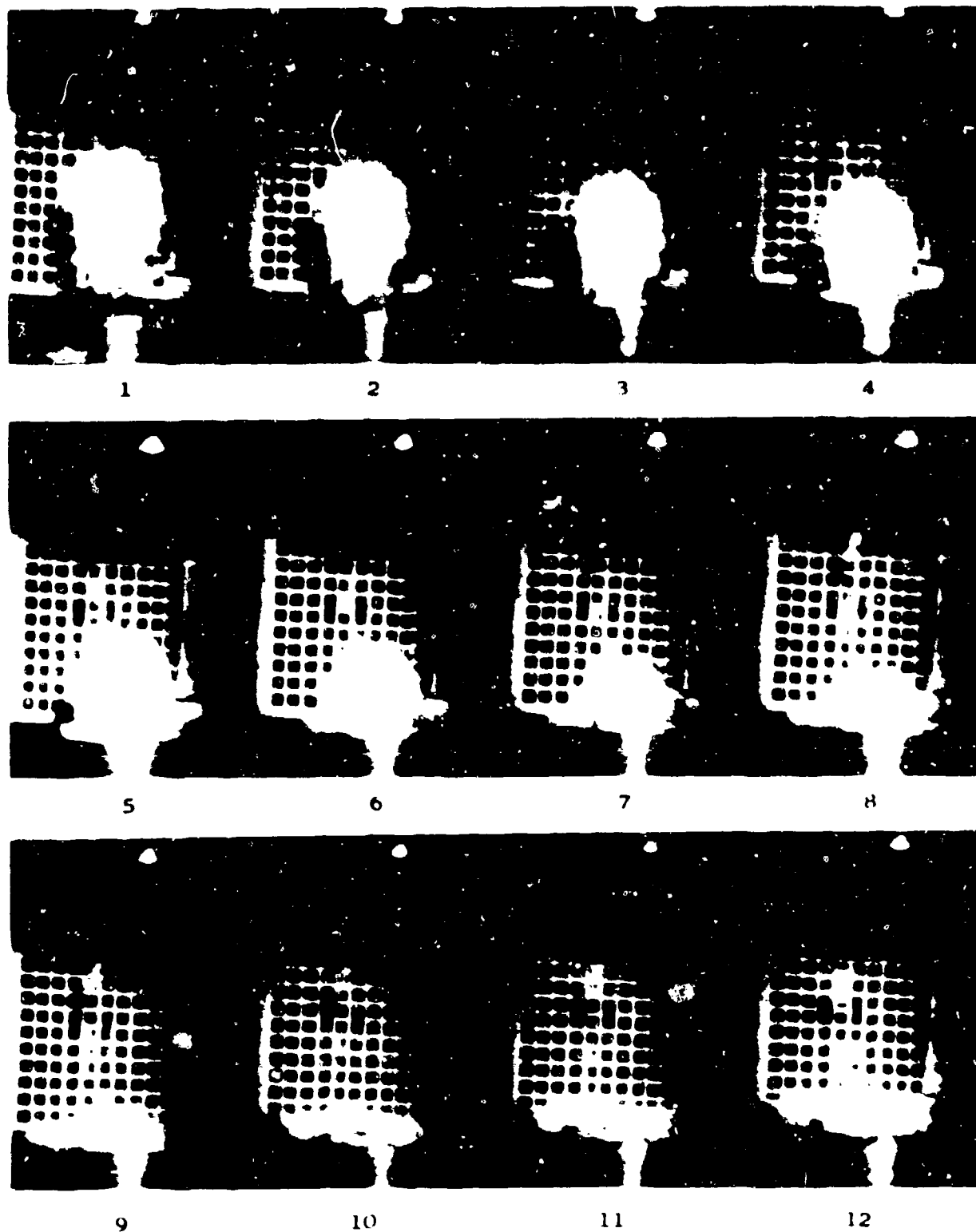
Figure 7. Cine photographs of bird impacting rigid plate.
Shot no. 5150, velocity: 85 m/s, 7,500 frames/s

imparted to the plate should be only slightly greater than the original momentum of the bird.

ii)   The radial velocity of the bird debris was measured from the photographs and a typical ratio of exit to impact velocity was 0.6. This indicates that kinetic energy was lost during impact and probably went into destruction of the bird.

iii)   The bird debris exited from the impact in a well defined, axially symetric "doghnut" of material. Feathers at high speed often preceded the main body of the bird but carried very little of the energy or momentum of the impact.

2.4.3   Pressure Measurement

The work described in this report was a preliminary study for a program designed to investigate the impact loading of aircraft windshields during collision with birds. To aid in cha   cterization of the bird during impact, a number of experiments were conducted to measure the time and radial variations of the pressure generated by birds impacting a rigid plate.

Apparently, there are no transducers commercially available specifically designed for measuring impact pressure of the nature described in this report. Listed below are some considerations governing transducer selection:

i)   The transducer must be small enough to permit the close packing necessary to obtain adequate radial resolution of the pressure (e.g., 1.27 cm between centers).

ii)   The transducer must be acceleration compensated to minimize spurious signals generated by high plate accelerations.

iii)   The transducer must have a linear response up to a minimum pressure of 345 MN/m^2 (50,000 psi), a typical maximum pressure expected.

iv)   The transducer must sense only unidirectional pressure (along the trajectory axis).

15

v)   The transducer must have adequate bandwidth
     to detect significant transient pressures (of the
     order of 100 kHz).

vi) The transducer must be rugged enough to
     withstand the high acceleration loadings
     expected during impact.

Piezoelectric quartz pressure transducers fulfill most of these
requirements and have been in common use for measurement of pneumatic
and hydraulic pressures for many years. When pressure is applied on
the quartz crystal, a voltage (and charge) proportional to the pressure is
generated on the crystal. The crystal behaves as a voltage source of
extremely high output impedance and it is therefore necessary to
measure the generated voltage with an instrument possessing even
greater input impedance. A high effective input impedance is obtained
by inserting a charge amplifier or impedance converter between the
crystal and the measuring device as shown in Figure 8. The charge
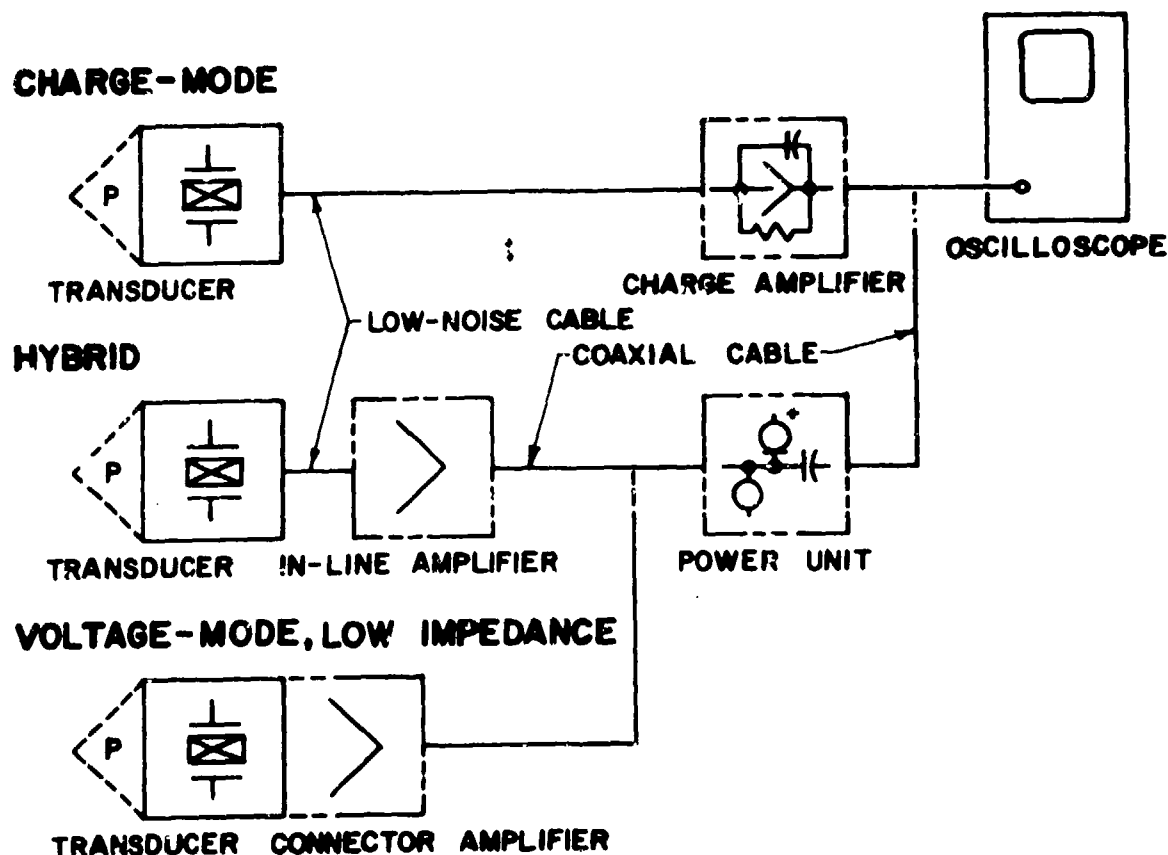
Figure 8. Configurations for the use of quartz crystal
            pressure transducers.

amplifier or impedance converter usually has a voltage gain of unity, an extremely high input impedance and an output impedance of the order of 50 ohms, thus drawing extremely small current from the crystal but capable of delivering measurable current to the monitoring equipment.

There are basically two configurations of the crystal and impedance converter system. In the first type (charge-mode and Hybrid of Figure 8) the crystal is connected to the impedance converter/charge amplifier by a high impedance line, which is sensitive to electrical noise pickup. The older type (charge-mode) has a large, completely separate charge amplifier and is particularly noise sensitive. The newer type (Hybrid) employs a compact impedance converter physically located in the coaxial line close to the crystal, thus decreasing the length of high impedance line and associated noise sensitivity. In order to eliminate the noise pickup problem, the second type (voltage-mode in Figure 8) has been developed in which the impedance converter is physically located in the transducer housing, thus reducing the length of high impedance, noise sensitive line to essentially zero.

The first transducers chosen (Kistler 207C3) contained built-in converters. A Kistler Type 587D coupler/power supply was used in conjunction with each transducer. The couplers were normalized with the transducers and cables at the factory and the couplers were set for unity gain. The output of each coupler/power supply was a/c coupled to a Tektronics 1A7A preamplifier, with built-in low pass filter, for display on a dual trace oscilloscope. For each shot, the output filtered with the low pass filter (-3 db point at 10 kHz) and the unfiltered output were displayed as separate traces on the same oscillograph.

A calibration method for the transducers was developed to verify the applicability of the manufacturer's calibration data to the unidirectional loads anticipated (Appendix D). A device was fabricated to enable unidirectional axial loads similar to those expected in service to be applied to the transducer and measurements were taken

17

to determine the response of the transducer. It was found that the
unidirectional calibration obtained was essentially identical to the
separately measured hydrostatic calibration. The manufacturer's
linearity and range specifications were checked and found to be
adequate. A quasidynamic calibration using a 1 Hz square wave was
also carried out as a check on damping and frequency response. It
was concluded that the transducers could be expected to provide
reliable, accurate pressure data over the range of pressures and
frequencies expected.

The transducers were flush mounted at 1.27 cm radial intervals in
a 5.10 cm thick, 15.25 cm diameter 4340 steel target disk(Figure 9), heat treated

Figure 9. Target disk showing mounting arrangement
and transducer placement.

to a yield strength of 1035 MN/m^2 (150,000 psi) and Rockwell C45. The disk was supported by a 10.16 cm diameter, 1.27 cm wall tube, machine seated and welded to a 3.81 cm thick flange. This fixture could be mounted inside the target tank on the 3.81 cm thick wall of the tank, or outside the target tank and secured to the tank wall by six, 1.90 cm diameter bolts. The purpose of the design was to provide a rigid target support while permitting ease of access to the transducers.

A series of bird impacts on the instrumented target was conducted and the original set of transducers began to malfunction after ten impacts; the transducers mounted off center failing first. An investigation of the target revealed that the transducers were not flush mounted but protruded out of the face of the disk by approximately 0.075 cm. It was suspected that the lateral flow of bird debris was side loading the transducer, resulting in debonding of the quartz crystal and subsequent failure. A new plate was machined with care taken to obtain concentricity of the mounting threads with the body of the crystal, 0.00127 cm radial clearance at the forward end, and the end recessed 0.005 cm below the plate surface.

Transducer failure continued to be a problem but it occurred less frequently than with the original plate. Eight transducers were destroyed during the first 162 impacts. Although the manufacturer was sharing part of the expense, it had become clear that the cost of transducer replacement would be prohibitive for a long term program. Accordingly, a comparison program and shock investigation was conducted as described in Appendix D. For this program an accelerometer to measure acceleration loadings and a PCB 108 series piezotron transducer* (with self contained charge converter) for reliability comparison with two PCB 118 series transducers* (with inline charge converters) were obtained. The PCB 108 transducer failed after 47 shots, probably due to spallation of the epoxy used to mount the impedance converter in

* Manufactured by PCB Piezotronics Corporation.

the case. Although accelerations of 600,000 to 800,000 m/s^2 (60,000 to 80,000 "g's") at up to 200 kHz persisting for hundreds of cycles were regularly monitored during the test series, the two PCB 118 transducers performed satisfactorily for 71 shots and displayed no indications of imminent failure.

SECTION 3

EXPERIMENTAL RESULTS

A relatively large experimental program was undertaken to develop launch techniques for small birds and to develop instrumentation capability (photographic, x-radiographic, velocity measurement, and pressure measurement). Approximately 150 shots were involved in this phase of the program. After the experimental capability was established and verified, effort was concentrated on obtaining pressure data as outlined in Table 1.

3.1 CENTER-OF-IMPACT PRESSURE TIME DATA

Pressure on the impact plate during bird impacts was measured as outlined in Section 2.4.3, in an effort to describe the manner in which a bird loads a plate during impact. The output from pressure transducers mounted in the impact plate were recorded on oscilloscopes and typical records from the impact center line are shown in Figure 10. A more complete selection of this data is presented in Appendix E. Pressures up to 100 MN/m^2 and pressure durations of the order of hundreds of microseconds are typical.

The pressure time records could be described as a relatively low frequency "base" pressure on which was superimposed a high frequency pressure variation as illustrated in Figure 11. The base pressure profile remained similar from shot to shot, although amplitude and duration varied with velocity and bird size. The high frequency component varied in frequency and amplitude from shot to shot and appeared to have little repeatable structure. Acceleration measurements were taken on the transducer plate to determine the magnitude of the shock loading of the transducers. The high frequency pressure component could have been "noise" produced by the inability of the acceleration compensation in the pressure transducers to adequately reject high amplitude, high frequency shock accelerations. A number

21

TABLE 1. BIRD IMPACT PRESSURE DATA

SHOT	BIRD MASS (kg)	VELOCITY (m/s)	TRANSDUCER POSITION	PEAK PRESSURE (MN/m^2)	PULSE DURATION (μs)	RISE TIME (μs)	IMPULSE INTENSITY* (kNs/m^2)
4946	.053	178	A	40.7	420		8.05
4947	.1.8	187	A	57.1	470		
4948	.112	161	A	50.1	560	80	8.05
4948	.112	161	B	33.8	560	40	8.34
4949	.110	163	A	37.6	600	115	7.42
4949	.110	163	B	25.6	600	160	7.36
4950	.109	196	A	53.2	455	135	10.61
4951	.069	215	A	56.5	380	60	10.92
4954	.096	66.4	A				1.77
4962	.065	253	A	78.3		30	
4963	.065	154	A	45.4	520	10	6.69
4964	.074	204	A	62.6	470	50	11.87
4965	.060	201	A	70.3	380	35	9.59
4968	.066	46.3	A	3.4			
4970	.067	62.8	A	4.7			
4971	.072	96.9	A	17.6			
4972	.076	64.3	A	7.9			
4973	.117	229	A	75.8	370	45	13.77
4985	.115	71.8	A	6.4			
4986	.114	71.0	B	4.7			
4987	.117	105	B	15.6	900	25	2.99
4988	.116	52.7	B	2.4		75	
4989	.110	128	B	15.6		80	
4990	.098	114	B	22.7	380	8	4.01
4991	.106	138	B	10.5	370	30	3.50
4992	.109	119	B	25.1	420	14	2.65
4993	.081	159	B	37.5	320	32	4.07
4995	.081	197	B	32.8	250	60	4.48
4996	114	274	B	59.2	460	22	9.75
5003	.064	97.2	A	30.4		145	
5003	.064	97.2	B	14.4		120	
5006	.057	327	A	62.6	370	120	
5006	.057	327	B	50.1	300	10	
5007	.060	277	A		360	15	11.99
5007	.060	277	B	53.6	310	25	7.80
5008	.051	262	A		330	12	8.99

NOTE: Positions; A-center of impact, B-1.27 cm off center, C-2.54 cm off center, D-3.81 cm off center.

* Impulse intensity (I_I) is defined as $I_I = \int P dt$.

TABLE 1 (cont'd.)

SHOT	BIRD MASS (kg)	VELOCITY (m/s)	TRANSDUCER POSITION	PEAK PRESSURE (MN/m^2)	PULSE DURATION (μs)	RISE TIME (μs)	IMPULSE INTENSITY* (kNs/m^2)
5008	.051	262	B	45.9	330	35	7.51
5057	.050	123	B	7.9	700	28	2.18
5058	.064	154	B	14.1	640	65	5.43
5059	.066	92.0	B	7.2	750	70	2.43
5078	.17	77.4	C	6.2			
5079	.110	79.8	C	5.0			
5081	.115	94.1	C	4.3	650	100	
5082	.113	127	C	8.3	430	50	1.86
5083	.114	129	C	8.7	440	40	2.18
5108	.103	159	C	10.3	420	115	2.81
5110	.102	167**	A	25.8	710		8.52
5110	.102	167**	C	4.4	590		2.02
5111	.086	142	A	33.6	670	95	7.58
5111	.086	142	C	10.2	470	150	3.03
5113	.107	22**	A	36.0	710	65	
5113	.107	22**	C	18.0	560	27	
5114	.094	38**	A	33.6	620	85	
5118	.098	93**	A	42.2	590	130	10.89
5121	.100	236**	A	69.6	640	155	
5121	.100	236**	C	18.6	540	110	11.34
5122	.102	16?	A	43.2	640	90	12.47
5122	.102	169	C	18.0	560	10	5.21
5123	.075	?	A	18.0	630	35	
5123	.075	143	C	11.3	540	180	
5124	.058	158	A	38.4	550	75	7.89
5125	.071	200**	A	72.0	500	40	10.64
5125	.071	200**	C	15.8	480	40	4.26
5126	.074	198	A	41.0	485	45	9.32
5126	.074	198	B	29.9	475	20	6.56
5126	.074	198	C	13.5	470	140	
5127	.078	196	A	64.8	580	65	11.14
5127	.078	196	B		540		
5127	.078	196	C	24.8	510	250	6.63
5129	.108	60**	A	6.7	600		15.06
5129	.108	60**	B	5.9			
5129	.108	60**	C	2.7	610		9.66

NOTE: Positions; A-center of impact, B-1.27 cm off center, C-2.54 cm off center, D-3.81 cm off center.

* Impulse intensity (I_I) is defined as $I_I = \int Pdt$.

** Velocity was estimated from powder loading curve.

TABLE 1 (cont'd.)

| SHOT	BIRD MASS (kg)	VELOCITY (m/s)	TRANSDUCER POSITION	PEAK PRESSURE (MN/m²)	PULSE DURATION (μs)	RISE TIME (μs)	IMPULSE INTENSITY* (kNs/m²)
5131	.148	198**	A	50.9	800	200	16.73
5131	.148	198**	C	23.5	590	150	10.11
5133	.065	104	A	22.8		35	
5133	.065	104	C	4.5			
5134	.124	167**	A	33.1		115	
5134	.124	167**	B	33.6		235	
5134	.124	167**	C	14.6			
5136	.105	202	A	59.5	700		
5136	.105	202	B		450		
5136	.105	202	C	24.8	340		5.37
5139	.089	148	A	36.0	740		7.89
5139	.089	148	B	26.3			7.42
5139	.089	148	C	17.3	590		4.93
5140	.126	152**	A	26.6	900		9.73
5140	.126	152**	B	19.9	800		5.56
5140	.126	152**	C	9.0	830		5.49
5141	.132	171	A	30.0			
5141	.132	171	B	24.9			
5141	.132	171	C	7.9			
5144	.107	144	A	27.7	880		7.58
5144	.107	144	B	17.9	870	125	6.88
5144	.107	144	C	9.0			4.23
5145	.112	128	A	19.8			
5145	.112	128	B	26.5			
5145	.112	128	C	8.1			
5146	.094	73.7	A	8.1			
5147	.112	110	C	6.0			
5149	.102	88.9	B	12.0			
5149	.102	88.9	C	5.2			
5149	.102	88 9	D	.4			
5150	.096	85.0**	B	6.9			
5150	.096	85.0**	C	2.7			
5154	.067	139	A				
5154	.067	139	B	17.4	540	35	5.21
5154	.067	139	C	7.9	490	225	2.21
5155	.066	112	A				

NOTE: Positions; A-center of impact, B-1.27 cm off center, C-2.54 cm off center, D-3.81 cm off center.
* Impulse intensity (I_I) is defined as $I_I = \int P dt$.
** Velocity was estimated from powder loading curve.

TABLE 1 (cont'd)

SHOT	BIRD MASS (kg)	VELOCITY (m/s)	TRANSDUCER POSITION	PEAK PRESSURE (MN/m^2)	PULSE DURATION (μs)	RISE TIME (μs)	IMPULSE INTENSITY* (kNs/m^2)
5155	.066	112	B	12.0	700	42	3.60
5155	.066	112	C	7.2	770	125	3.60
5157	.073	34.7	A	3.7			
5157	.073	34.7	B	1.7			
5167	.074	109	C	4.8	510		1.61
5170	.061	138	C	6.9	500		2.30
5171	.061	138	C	10.1	460		2.68
5172	.061	201**	C	13.2	380		2.58
5174	.099	168**	C	18.0	420	20	5.58
5174	.099	168**	C	3.7	410	120	0.82
5175	.101	164	C	12.3	600	20	5.15
5175	.101	164	D	8.3	580	300	2.97
5176	.092	112	C	4.7			
5178	.098	96.2	C	5.2			
5178	.098	96.2	D	4.6			
5180	.100	128**	D	1.1	780	130	.41
5181	.070	126	C	8.6	650	90	2.68
5181	.070	126	D	.5	600	250	0.17
5184	.103	305**	A	70.8	430	10	12.31
5184	.103	305**	C	2.9	360	50	
5187	.084	237	A		400	12	16.26
5187	.084	237	B		380	15	8.99
5190	.067	129	B		640		5.40
5191	.069	355	B		250		24.16
5192	.066	132	A				

NOTE: Positions; A-center of impact, B-1.27 cm off center, C-2.54 cm off center, D-3.81 cm off center.

* Impulse intensity (I_I) is defined as $I_I = \int Pdt$.

**Velocity was estimated from powder loading curve.
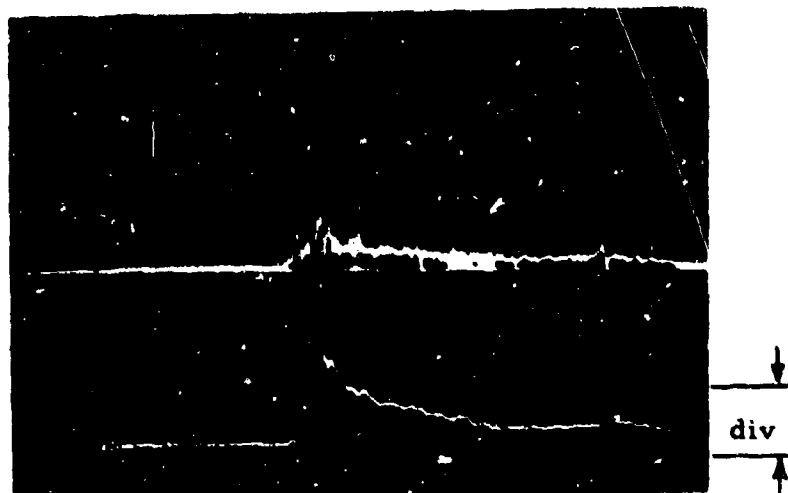
Shot no. 5129; 60 m/s, 4.95 MN/m^2/div
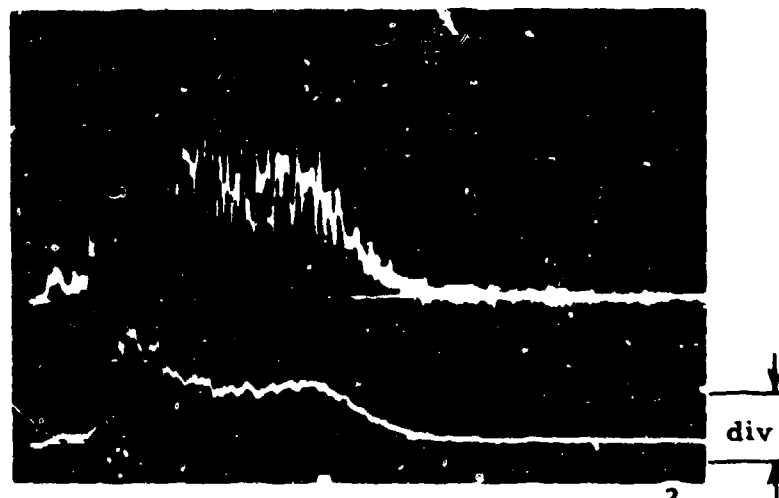
Shot no. 5126; 198 m/s, 24.78 MN/m^2/div
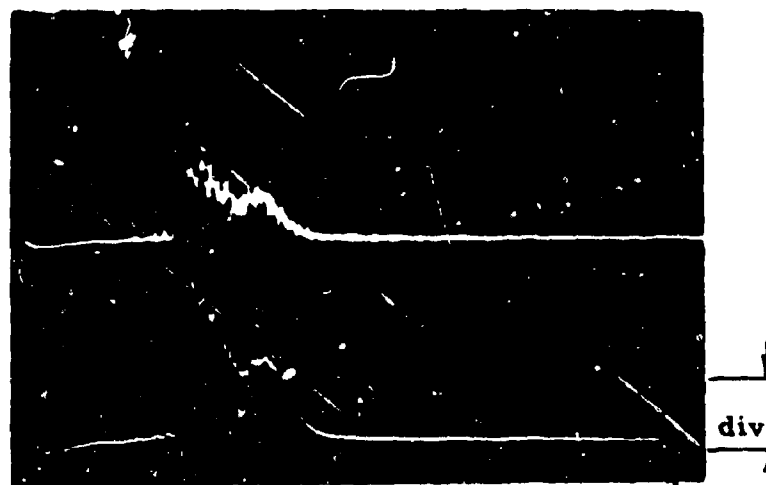
Shot no. 5187; 237 m/s, 24.78 MN/m^2/div

Figure 10. Center line pressure transducer outputs.
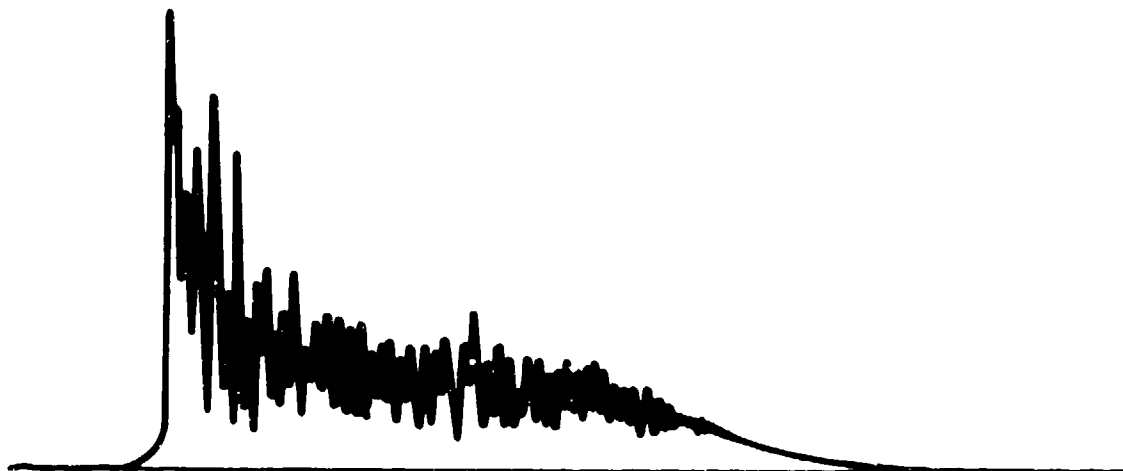
TYPICAL ₵ PRESSURE TRANSDUCER OUTPUT

BASE COMPONENT OF ₵ PRESSURE TRANSDUCER OUTPUT
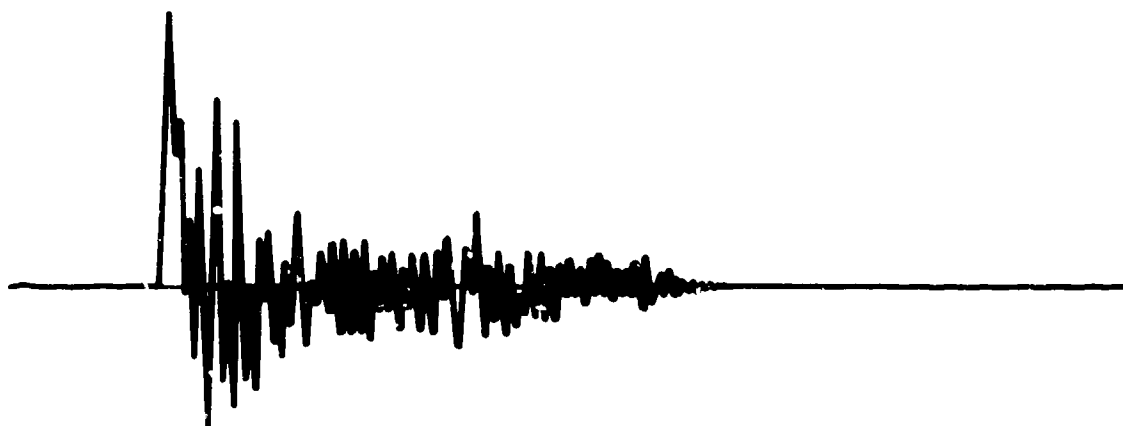
HIGH FREQUENCY PRESSURE VARIATION COMPONENT

Figure 11. Typical components of impact pressure
for real bird impacts.

of impacts with RTV "birds" produced similar accelerations to those
produced by real birds, but the RTV pressure data lacked the high
frequency content as indicated in Figure 12. The high frequency
pressure component of real bird impacts must therefore be regarded
as a particular and real characteristic of bird impacts and not just
instrumentation noise. This description of the center of impact
pressure time data suggests a simple bird model and it is instructive
to consider this model during the reduction of the raw data.

If the bulk of the bird is regarded as a homogeneous fluid-like
material characterized by some density and the physical dimensions
of the bird, then the unsteady flow of the bird material on the rigid
plate generates the base pressure observed. The shape of the base
pressure-time pulse is approximately that which could be expected
from the flow of a cylinder of homogeneous fluid of the length of the
bird. This is demonstrated by the similarity between the filtered
bird pressure trace and the RTV (homogeneous) body pressure trace
shown in Figure 12. The peak pressure generated is close to that
which might be expected from a fluid of specific gravity of approximately
unity.

The high frequency component of pressure may then be regarded
as the effect of inhomogeneites in the real bird. Local density
variations and/or large local material differences (for example bones)
in the bird could be the inhomogeneities responsible for the high
frequency pressure variations.

3.2   PRESSURE-TIME DATA

The mode of failure of a particular component such as an
aircraft windshield during impact will depend on the shape and material
of the component. For example, a thick component may not respond
grossly to the high frequency pressure variations of the impact load;
that is the component would be unable to deform in any gross manner
at high frequencies because of its size and material properties.

Bird impact; center line pressure transducer
unfiltered output; shot no. 5133; velocity 104 m/s
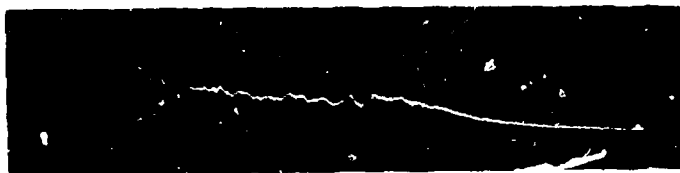
Bird impact; center line pressure transducer
filtered output; shot no. 5133; velocity 104 m/s

RTV-560 impact: center line pressure transducer unfiltered
output; shot no. 5075; velocity 77.4 m/s

Figure 12.   Pressure transducer output for real bird
and RTV 560 impacts.

The high frequency variation of the pressure would, therefore, be incapable of failing the component in flexure. However, it may cause delamination or spalling. For a typical windshield configuration with a thickness of the order of 3 cm and a sound speed of 2 mm/μs (Lexan), the double transit time across the material is approximately 30 μs and the material will not deform appreciably for frequencies above 10-20 kHz. It was, therefore, decided to filter the pressure data above 10 kHz and record the filtered pressure as the base pressure. As shown in Figure 10, filtering has removed most of the high frequency content and the base or low frequency pressure remains. Present considerations center on gross deformation of windshield materials and further analysis has been restricted to the filtered base pressure data. It must be noted that if other failure mechanisms are considered (e.g., delamination) or different components (e.g., fan blades), then the high frequency variations may be the important loading mechanism and any analysis will have to recognize this.

The following parameters were identified and extracted from the filtered or base pressure time data:

      i)   peak pressure - the maximum pressure recorded during impact.

      ii)   pressure duration - measured by extending the maximum slopes of the rise and fall of pressure to the zero pressure base line.

      iii)   pressure onset time - time delay of pressure onset at radial transducers with respect to center transducer.

      iv)   time to peak pressure - time from onset of pressure at center line to peak pressure.

      v)   impulse intensity - the area under the pressure-time curve obtained by numerically integrating digitized data.

3.3   PEAK PRESSURE-VELOCITY RELATION

The peak recorded pressure is indicative of the magnitude of the load imposed on the target during impact and, as the pressure

time curves have a similar shape from shot to shot, provides a
convenient parameter for characterizing the pressure data. The peak
pressure generated on the center of impact was measured for a
large number of shots and is plotted in Figure 13 as a function of impact
velocity. The following observations from the plots are made:

i)   The peak pressure appears to be independent
         of bird size over the range of birds tested
         (60-150 g). This supports the fluid impact
         model of a bird in which the pressure depends
         only on density and velocity and not on the
         size of the bird.

ii)   The peak pressure has a general velocity
         squared dependence which also supports a
         basically fluid model of a bird.

iii)   There is considerable scatter in the data
         and this is attributed to non-repeatability
         of bird structure, orientation at impact and
         center of impact which are beyond experimental
         control.

3.4   PEAK PRESSURE RADIAL VARIATION

Pressure was measured and recorded off axis at three
radii, 1.27 cm, 2.54 cm, and 3.81 cm; examples are displayed in
Figure 14. Further selected samples are collected in Appendix E.
This data was filtered and reduced in a similar manner to the center
line data as reported in Section 3.2. Peak pressures are shown plotted
as a function of velocity in Figures 15, 16 and 17. From the data and the
plots the following observations emerge:

i)   The form of the pressure time response is
         the same as the center of impact data; that
         is, it consists of a base pressure on which is
         superimposed a high frequency component.
         The high frequency components have been
         filtered out for analytic purposes as explained
         previously.

ii)   Peak pressures are roughly dependent on the
         impact velocity squared in a similar manner to the
         center of impact data and consistent with a fluid
         bird model.
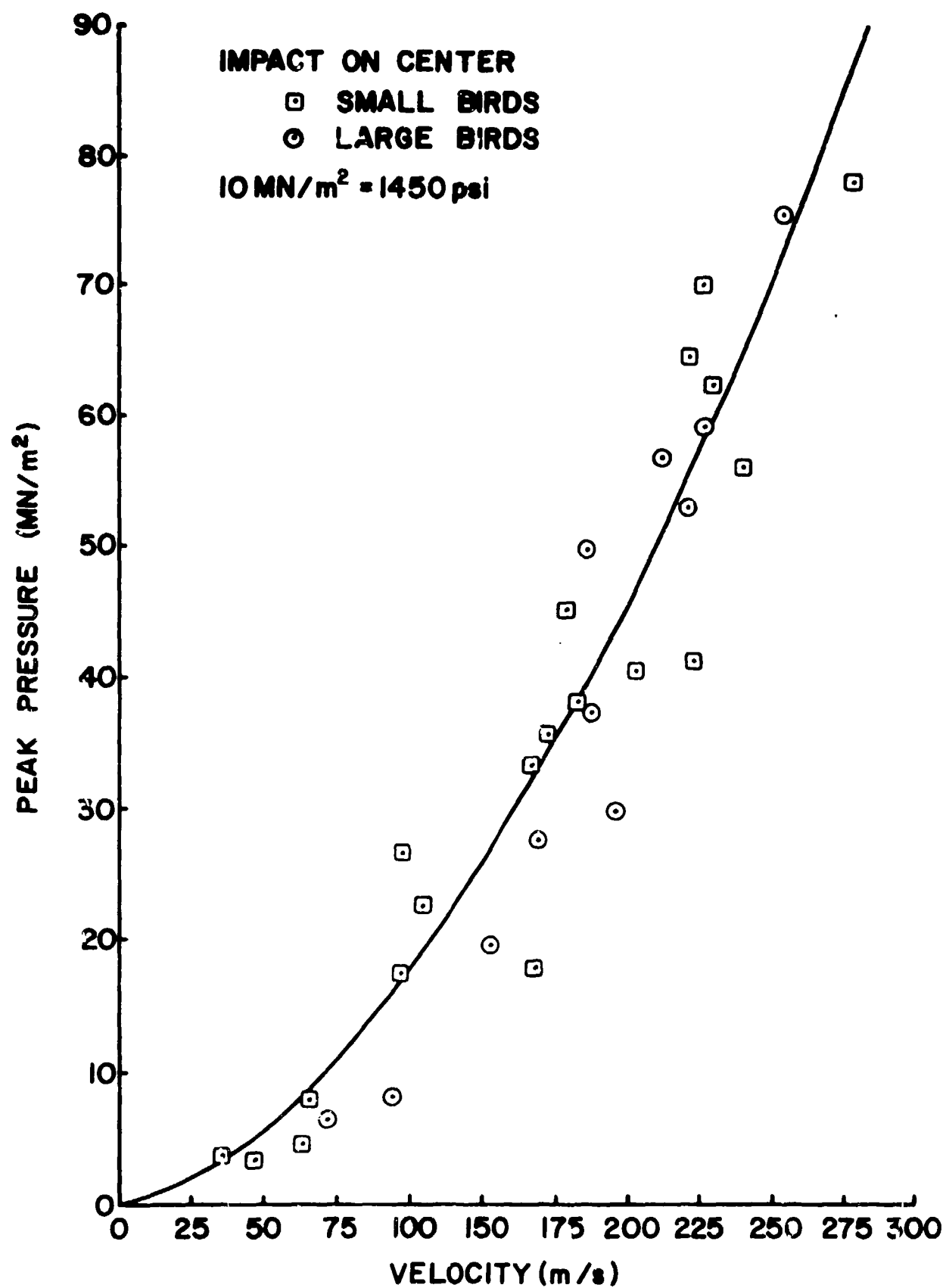
Figure 13.   Peak pressure versus impact velocity at center of impact.
The solid line is a least squares quadratic fit to the data.

AFFDL-TR-75-5
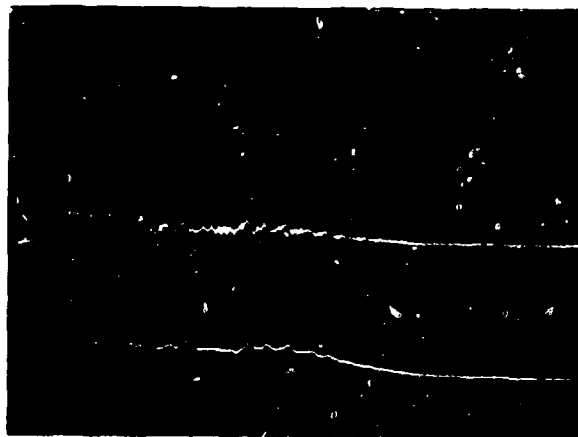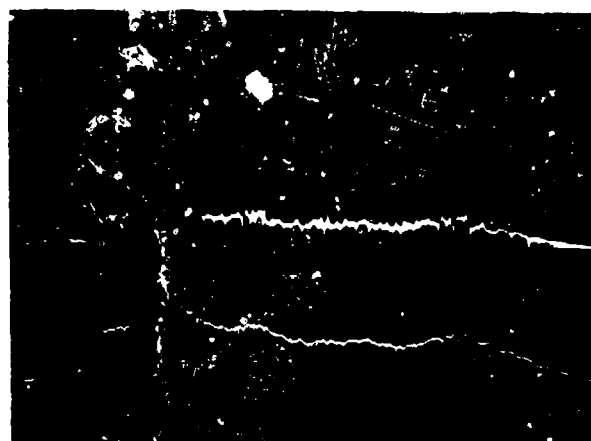
Shot no. 5139-A

Shot no. 5144-A
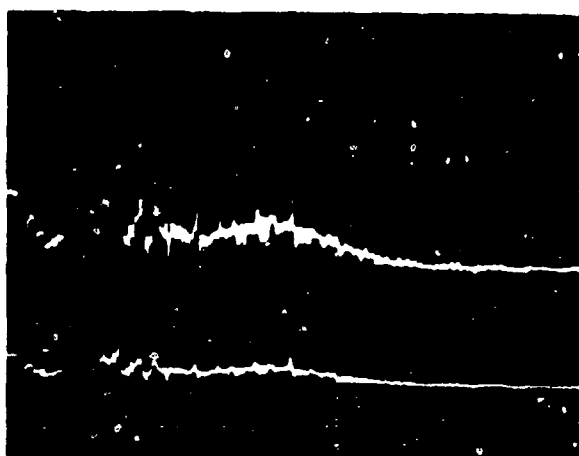
Shot no. 5129-B

Shot no. 5144-B
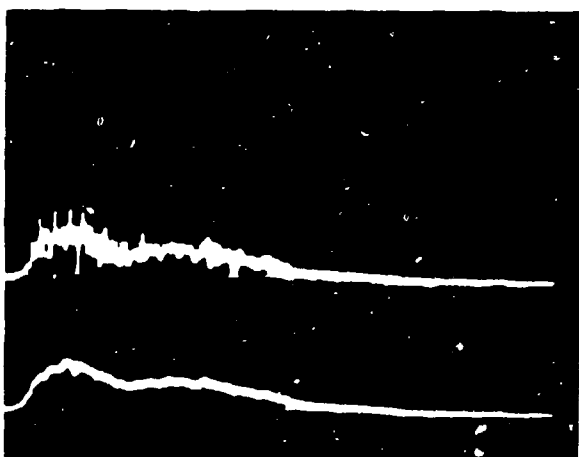
Shot no. 5129-C
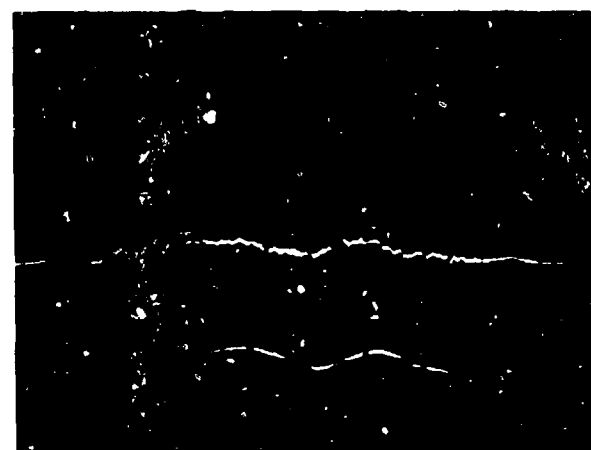
Shot no. 5144-C

Figure 14.   Pressure transducer outputs at transducer positions;
A-center of impact, B-1.27 cm off center and C-2.54 cm
off center.
Shot 5139 - 148 m/s, Shot 5144 - 144 m/s.

33
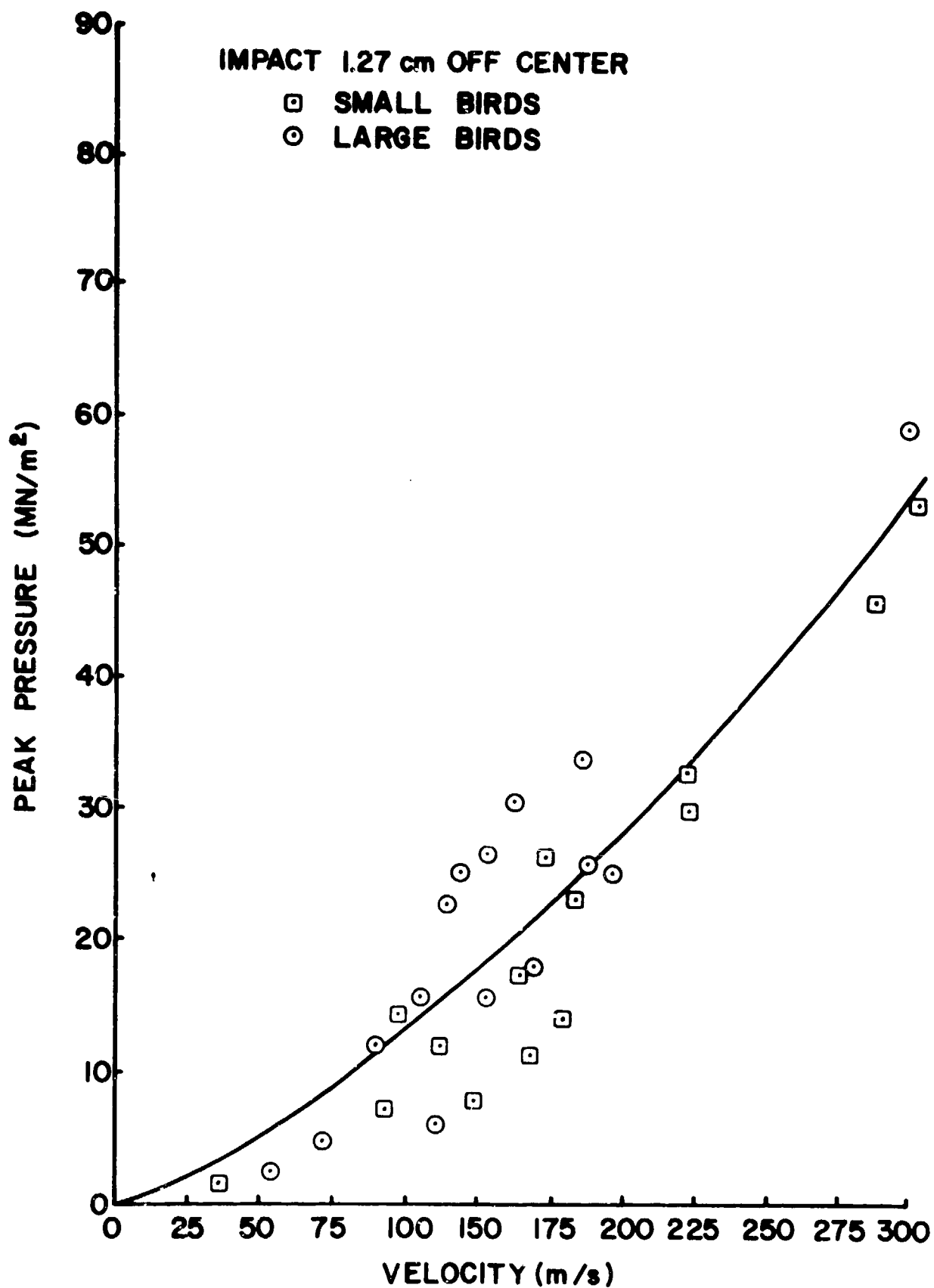
Figure 15. Peak pressure versus impact velocity 1.27 cm off center of impact. The solid line is a least squares quadratic fit to the data.
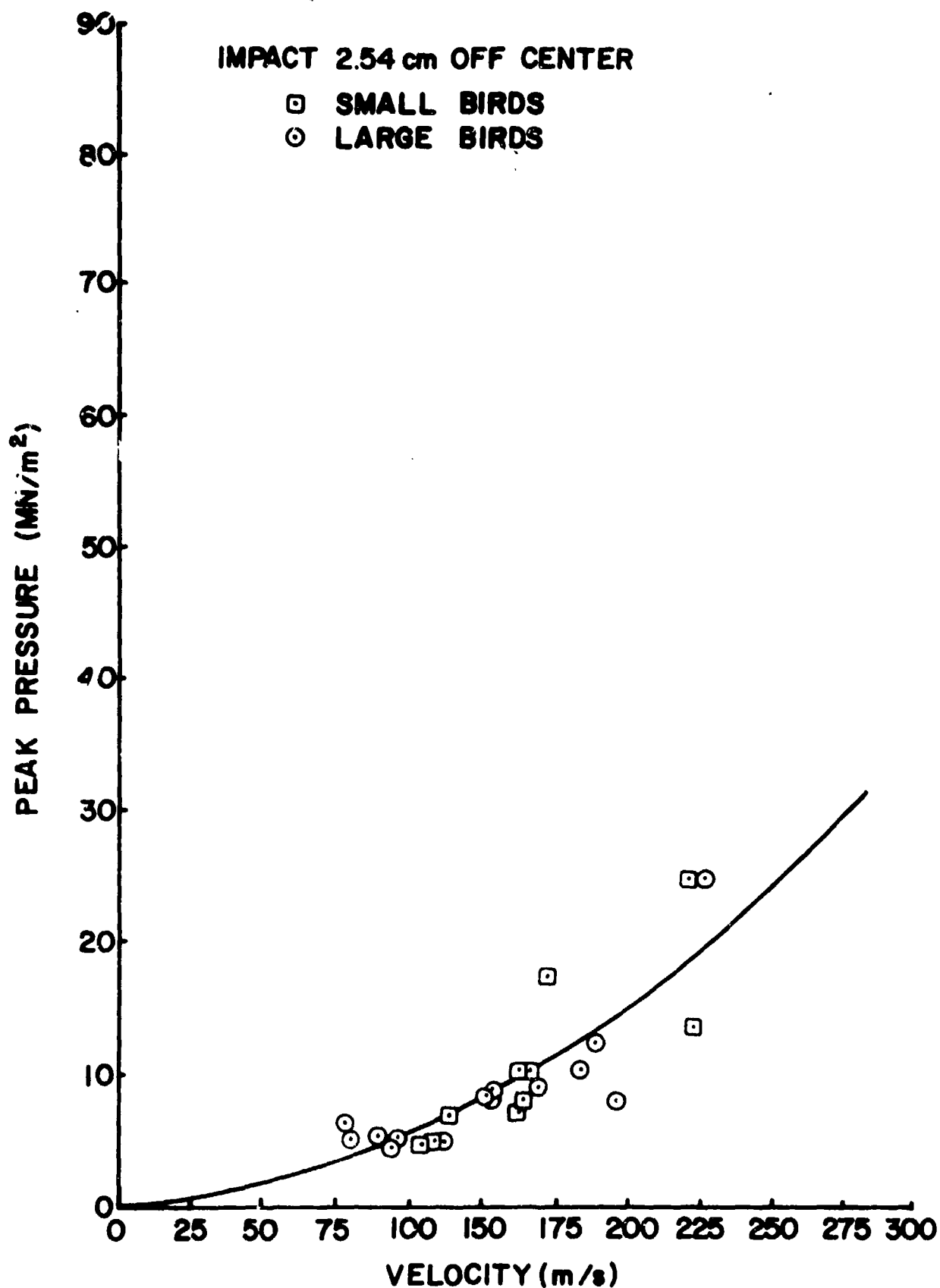
Figure 16. Peak pressure versus impact velocity 2. 54 cm off
center of impact. The solid line is a least squares
quadratic fit to the data.
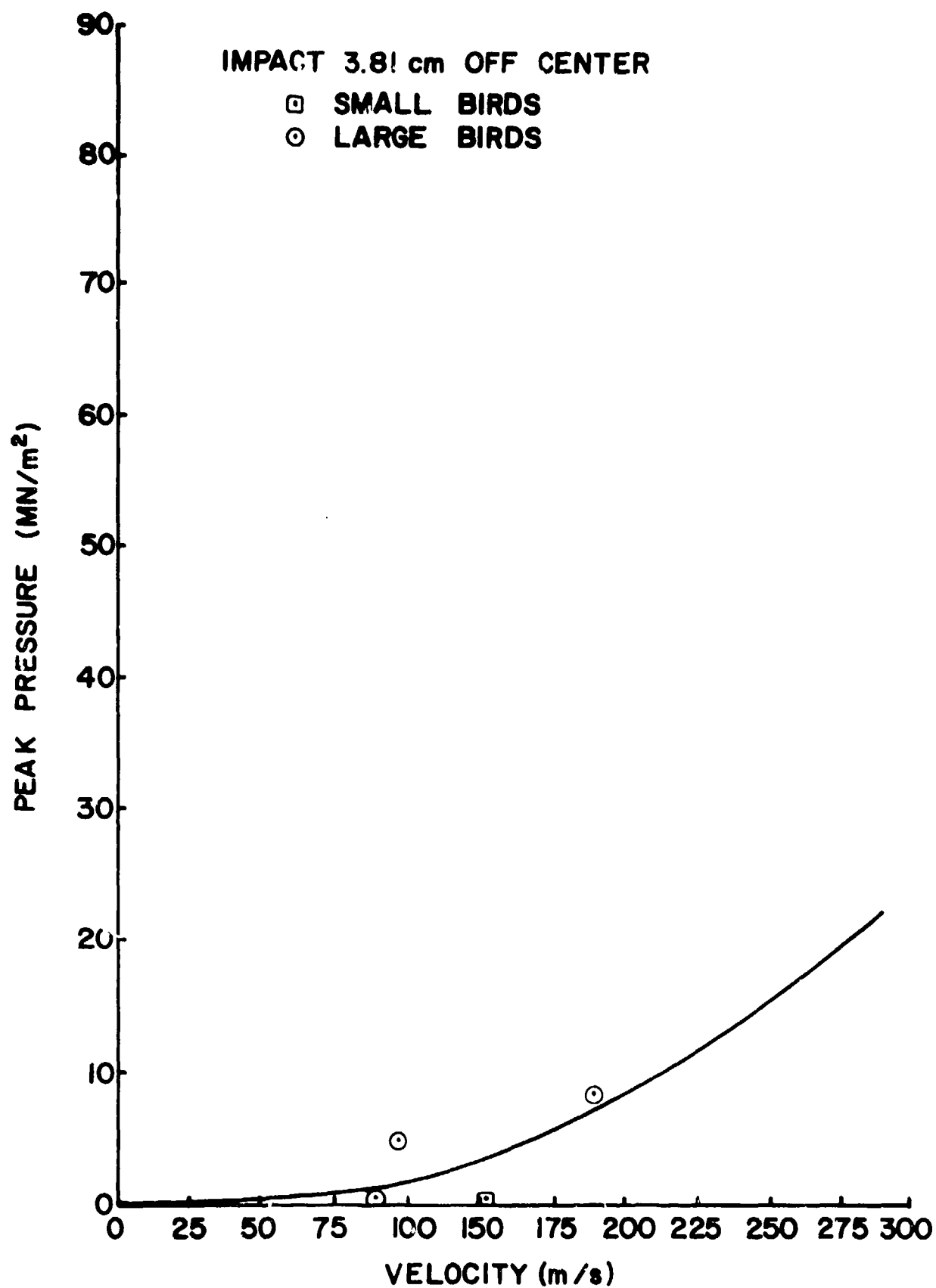
Figure 17.   Peak pressure versus impact velocity 3. 81 cm off
center of impact.   The solid line is a least squares
quadratic fit to the data.

iii)   Peak pressure falls with increasing radial
         distance from the center of impact, as shown
         in Figure 18.

iv)   Pressure onset time and time to peak pressure
         increase with increasing radial distance from
         the center of impact.

v)   Scatter in the data is comparable to that of
         the center line data and is similarly attributed
         to uncontrolled variations in bird structure,
         orientation and center of impact.

3.5   TIME INFORMATION AND IMPULSE INTENSITY

Measurements of pressure duration, onset time, time to peak
pressure and impulse intensity have just been initiated and only a
limited amount of data is available as yet. Impulse intensity is
defined as the integral of pressure with respect to time. Detailed
analysis of this data has not yet begun, however some preliminary
observations can he made:

i)   Onset time and time to peak pressure both
         increase with increasing radial distance from
         the center of impact.

ii)   Duration, onset time and time to peak pressure
         all decrease with increasing velocity.

iii)   Duration increases with increasing bird size.

iv)   Impulse intensity decreases with increasing
         radi   as i   ated in Figures 19, 20 and 21.

v)   Impulse intensity increases with bird mass and
         velocity as shown in Figure 19, 20 and 21.

vi)   Data scatter is large and is attributed to real and
         uncontrollabl   riations in bird structure,
         orientation :   . point of impact.
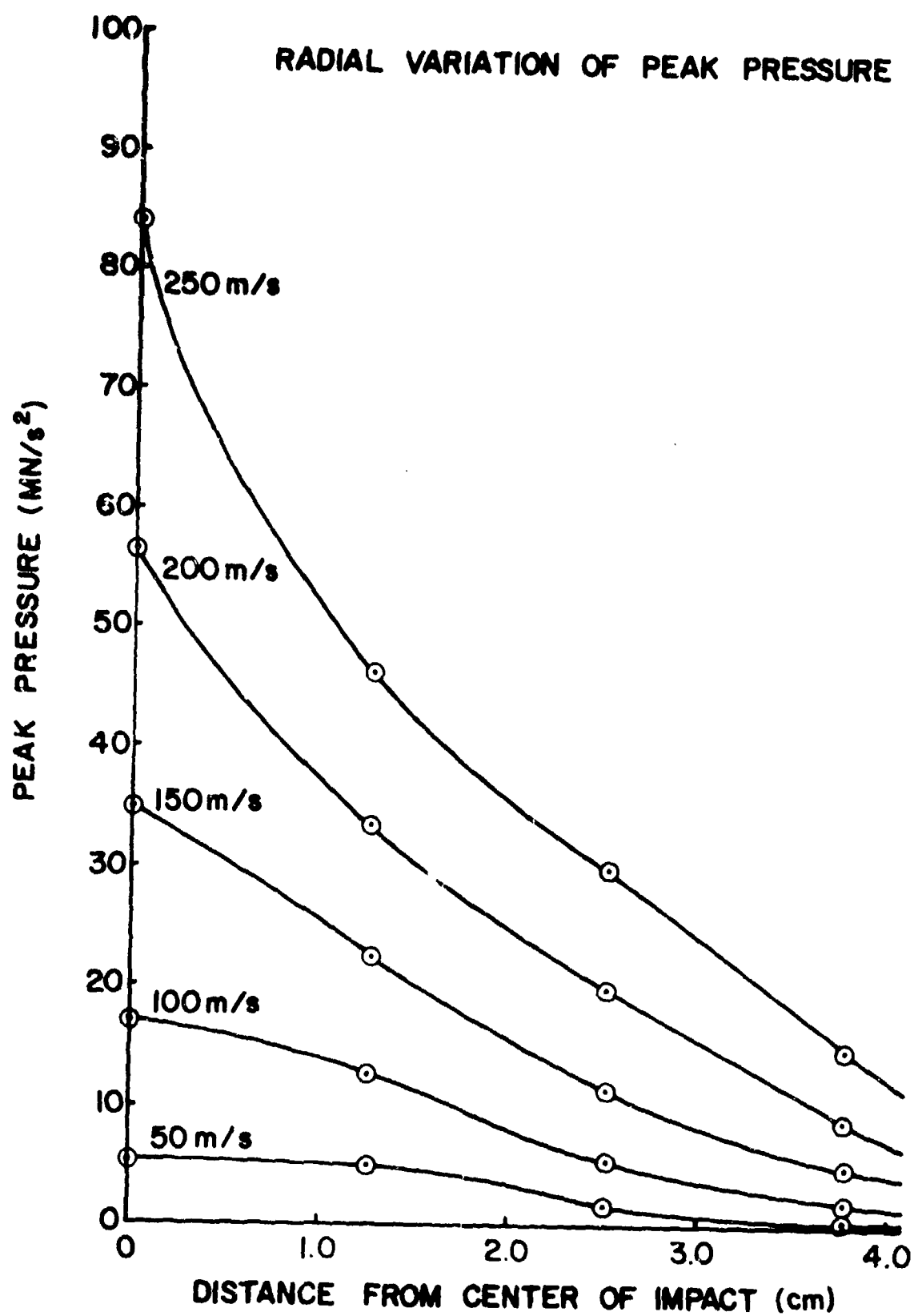
Figure 18. Peak pressure versus radial distance from
center of impact at selected impact velocities.
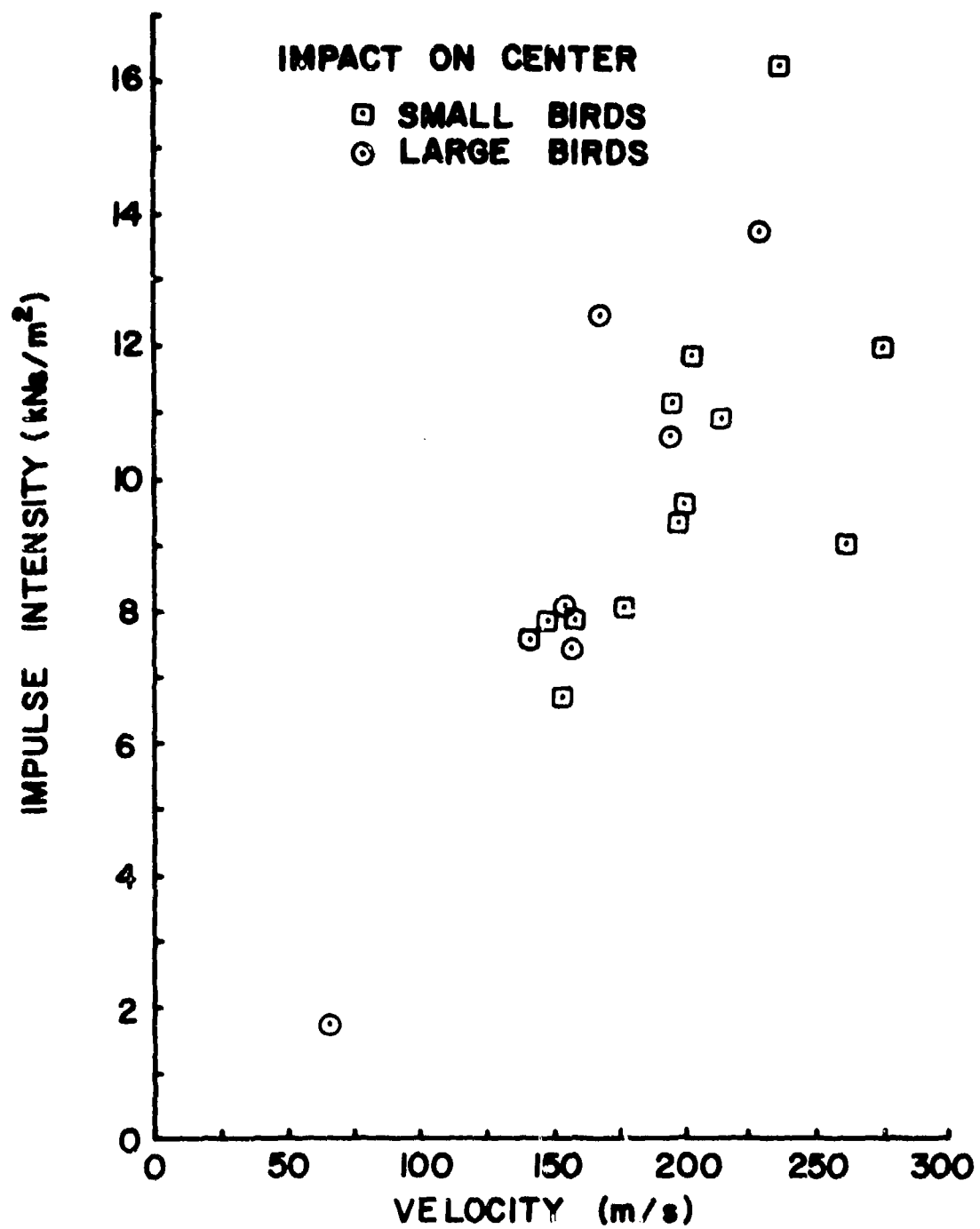
Figure 19. Impulse intensity ($\int$ Pdt) versus impact velocity at center of impact.
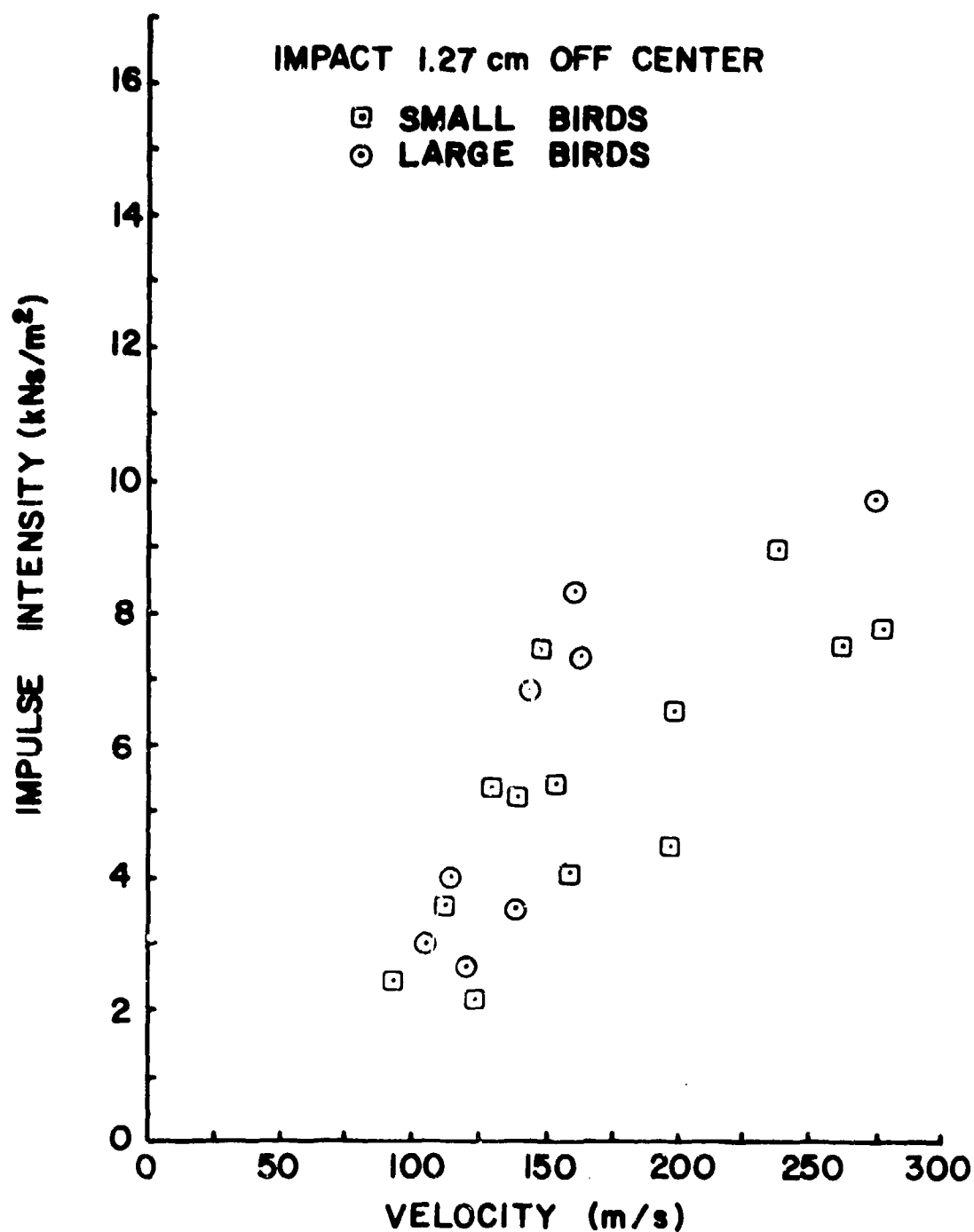
Figure 20. Impulse intensity ($\int$Pdt) versus impact velocity 1.27 cm off center of impact.
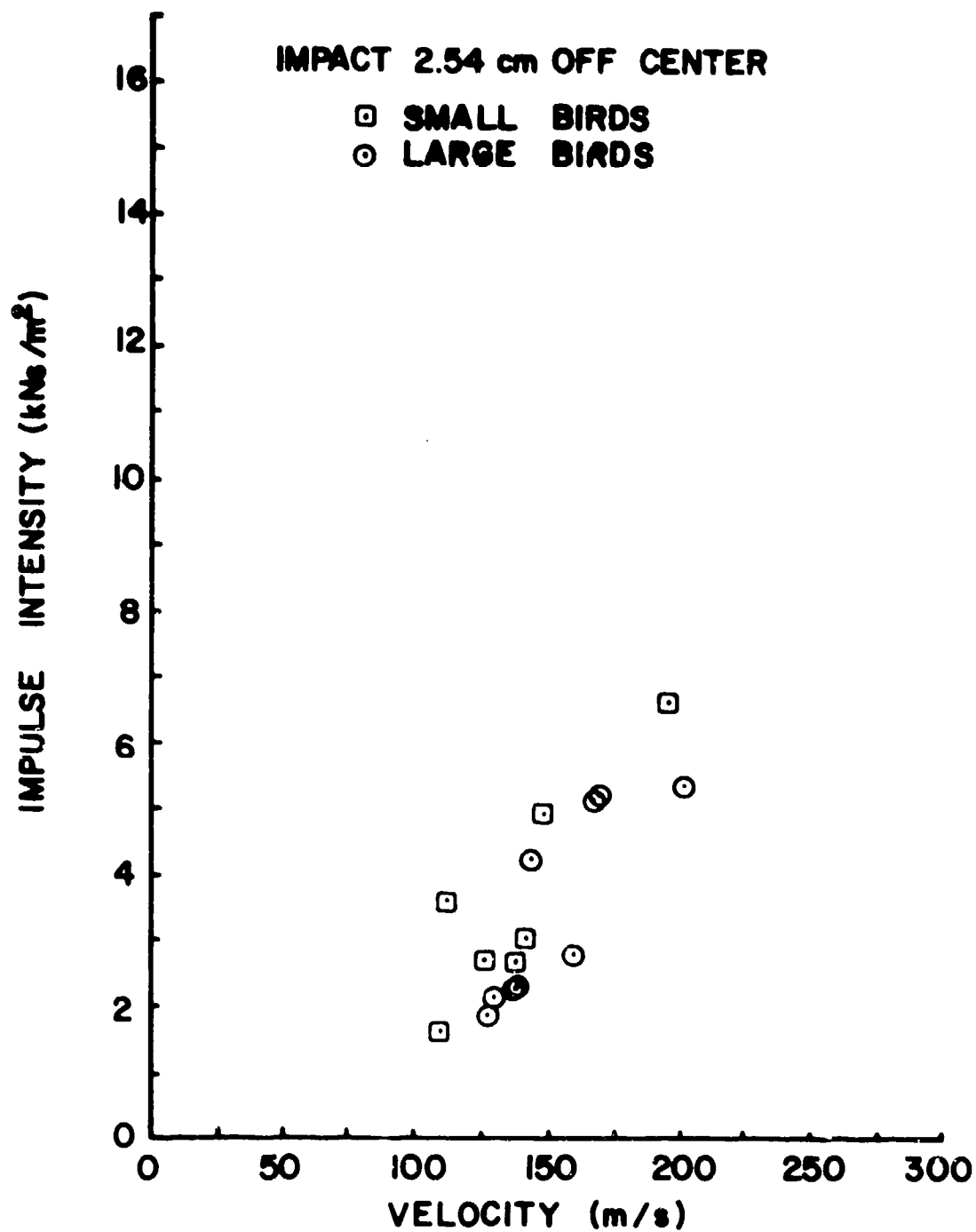
Figure 21. Impulse intensity ($\int$ Pdt) versus impact velocity
2. 54 cm off center of impact.

SECTION 4

DISCUSSION AND CONCLUSION

4.1   PRESSURE MEASUREMENTS

The pressure generated on a rigid plate by an impacting bird
has been characterized as a low frequency base pressure on which is
superimposed a high frequency pressure. It is suggested that the
base pressure can be explained with a homogeneous fluid bird model,
while the high frequency pressure "noise" arises from real bird
inhomogenieties, such as bones and local voids or density changes. In
support of this model it is noted that the peak base pressure obtained
by filtering the raw pressure data at 10 kHz, varies approximately
as velocity squared and is independent of bird size over the range of
parameters covered in these experiments (See Figure 13).

The measured radial variation of peak base pressure is shown
in Figure 18 and simply reflects the finite diameter of the bird. The
birds used in this study have effective diameters of approximately 3.20 cm
to 4.50 cm and should therefore generate little pressure at 2.54 cm or greater
off the axis of the impact. From Figure 18 it is apparent that the
pressure falls rapidly for radii over 2.54 cm although there is very little
data and considerable scatter in the data, due to off center impacts and
lack of axial bird symmetry. A slight dependence on bird size would
be expected in the radial variation of pressure. However such
variations would depend on bird diameter and bird diameter depends
approximately on the cube root of bird m.   . A variation of 60 g in bird
mass would therefore correspond to a variation of about 20% in radius.
For the birds considered here, the radius varies from smallest to
largest by about 0.65 cm which is 1/2 the spacing between transducers.
Detection of radial dependence of pressure on bird size will therefore be
unlikely for the range of bird sizes investigated in this report. This is
supported y the close grouping of large and small bird pressure data
in Figures 13, 15, 16 and 17.

42

SECTION 5
RECOMMENDATIONS

There are three recommendations that arise from the work reported herein and they are treated below:

i) Pressure data should be extended to impacts of larger birds. If the bird can be modeled as a fluid, the peak pressure would be independent of bird size and it does appear to be so over the range of masses employed in the present study (60-150 g). However, more confidence could be placed in a fluid model if size independence could be demonstrated up to 3 or 4 Kg birds. Impacts of larger birds would also clarify the dependence of pressure duration and pressure radial variations on bird size and aid in the generation of realistic boundary conditions for a fluid bird model.

ii) Development and formulation of a mathematical bird model should be continued. These present results indicate that it will be possible to describe the impact loading of birds impacted on rigid plates with a relatively simple mathematical model. This model could be extendable to flexible plates by substitution of the relative impact velocity (taking account of plate motion) for the impact velocity. Such a model, if successful, would greatly simplify the collection of design data and aid in the analysis of component response to bird impact.

iii) Development of a standardized realistic bird substitute should be undertaken. Sufficient data has been gathered on real birds (chickens) to permit a search for a realistic bird substitute which would generate, on the average, the same loading as a real bird at impact. The investigation and development of a substitute bird would produce the following results:

a) The investigations would greatly facilitate the development and verification of the bird model suggested in ii) above. The role that bones and other inhomogenieties play in the

pressure developed by real birds could be readily investigated using
substitute birds with various non-homogeneous compositions.

b) Real birds display an unsatisfactory
statistical scatter in the pressure data produced. This variation
reflects real and uncontrollable variations in bird structure and
orientation at impact. Such data scatter will become increasingly
difficult to accommodate as the structures impacted and the associated
response become more complicated and difficult to analyze. Every effort
should be made to eliminate sources of experimental loading uncertainty
when the response of real materials and components is investigated.
The problem of analyzing and predicting response will be difficult
enough without the added uncertainty of just what load was applied
in a given test. The development of a substitute bird, which could
be made with great precision and repeatability, could greatly reduce
data scatter and aid in the analysis of material responce.

c) Real birds, when impacted, present
experimental, aesthetic, and sanitary problems of non-trivial
dimensions. Significant range time must be expended to
maintain satisfactory sanitary standards on the range. A substitute
bird would, hopefully, be inanimate and a great deal easier to cope
with experimentally, thus freeing staff of an unpleasant and time
consuming duty.

APPENDIX A

X-RADIOGRAPHS OF LAUNCHED BIRDS
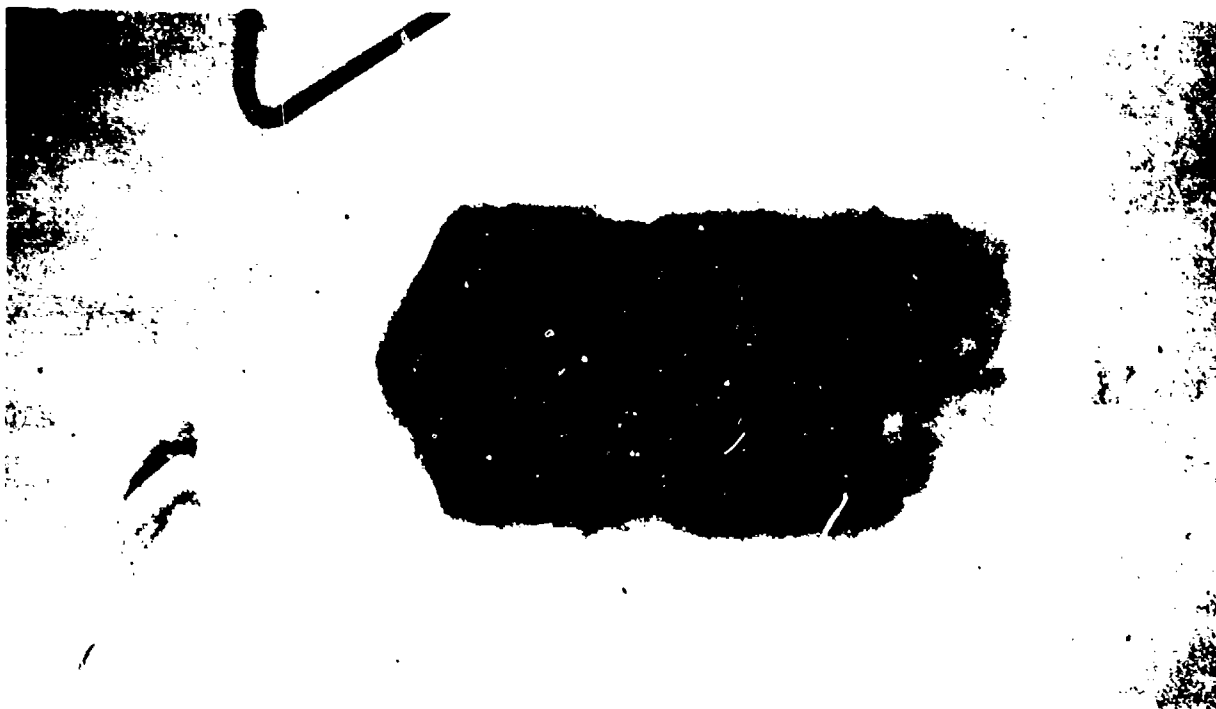
Shot No. 4946; velocity 178 m/s

Shot No. 4947; velocity 187 m/s
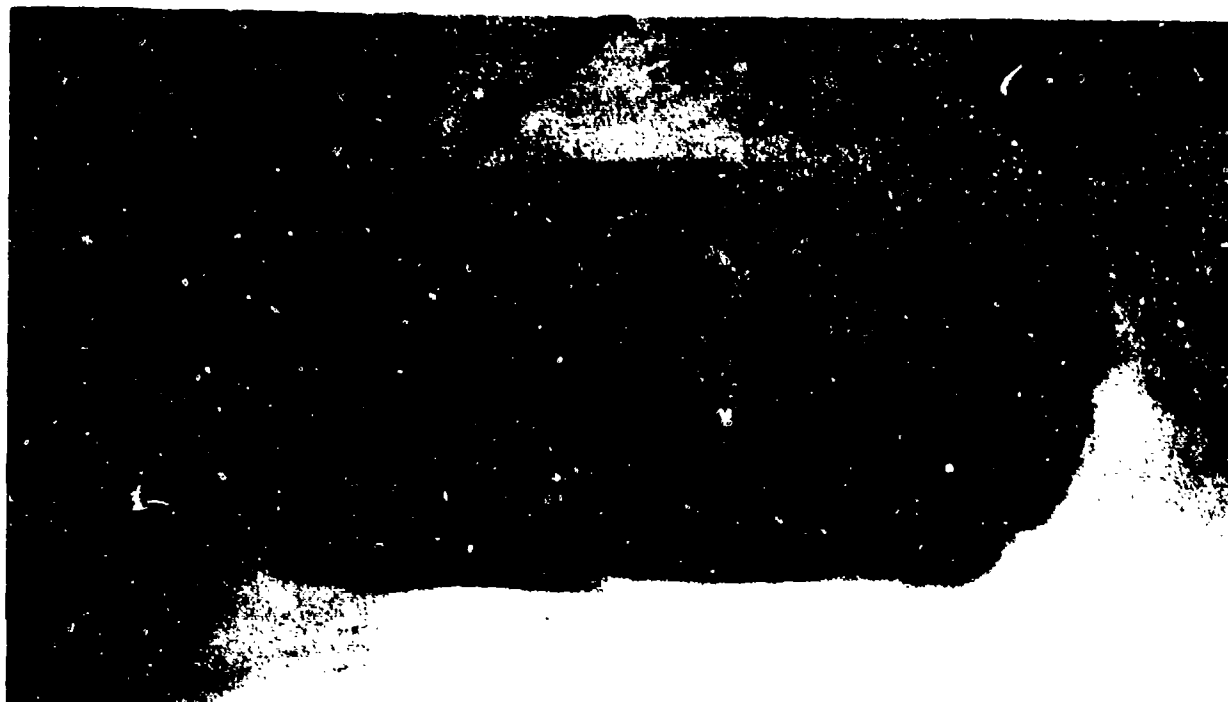
Shot No. 4948; velocity 161 m/s
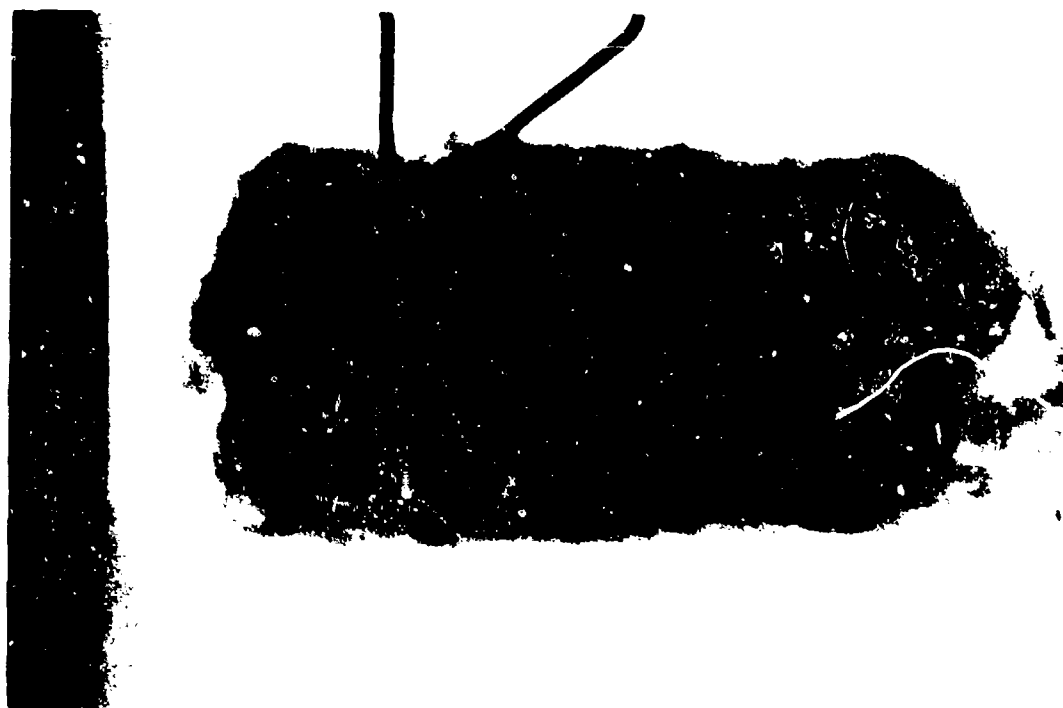
Shot No. 4949; velocity 163 m/s
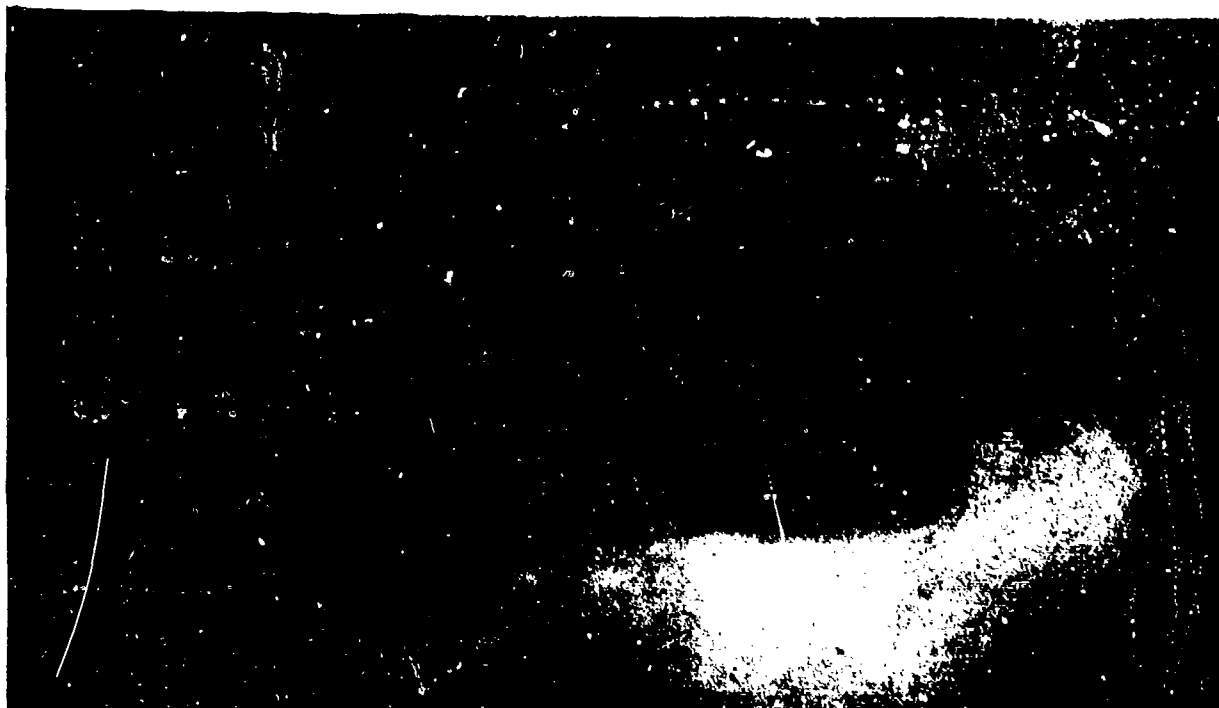
Shot No. 4951; velocity 215 m/s

Shot No. 4965; velocity 201 m/s

Shot No. 2986; velocity 71 m/s

Shot No. 4987; velocity 105 m/s

Shot No. 4989; velocity 128 m/s

Shot No. 4990; velocity 114 m/s

Shot No. 4991; velocity 138 m/s

Shot No. 5008; velocity 262 m/s

Shot No. 5176; velocity 112 m/s

Shot No. 5178; velocity 96.2 m/s

APPENDIX   B

PHOTOGRAPHS OF LAUNCHED BIRDS
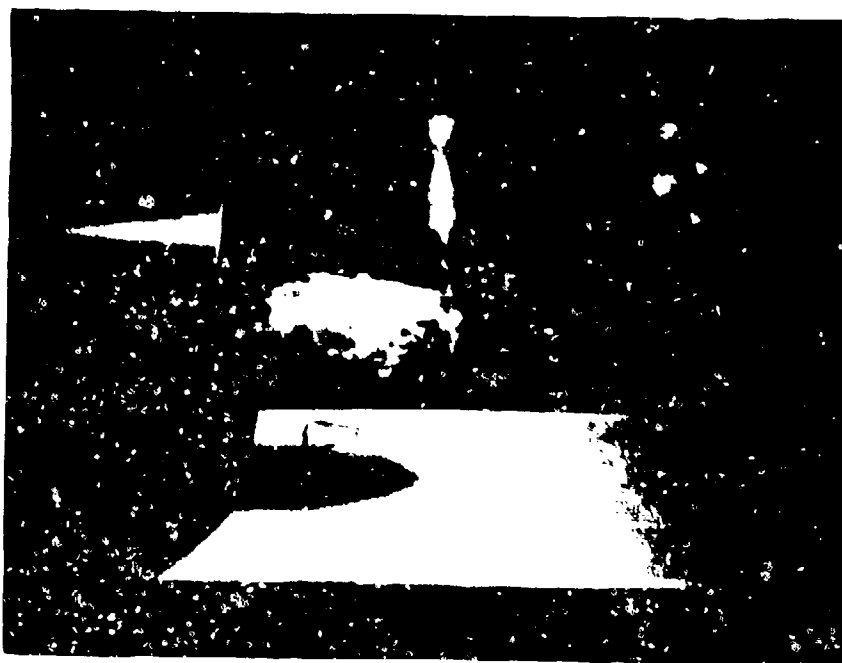
Shot No. 4947; velocity 187 m/s

Shot No. 4948; velocity 161 m/s

Shot No. 4949; velocity 163 m/s

Shot No. 4950; velocity 196 m/s
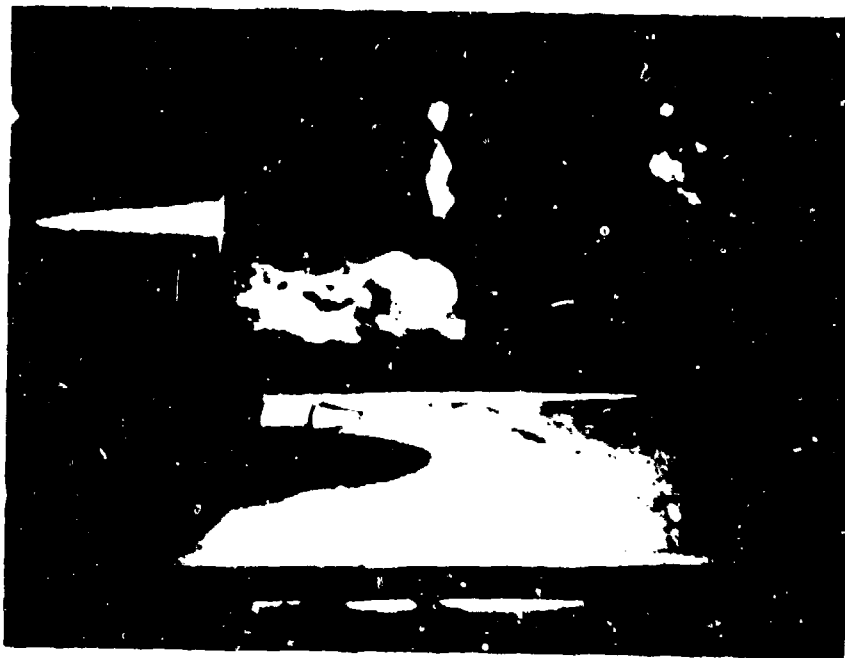
Shot No. 4954; velocity 66. 4 m/s

Shot No. 4963; velocity 154 m/s

Shot No. 4946; velocity 204 m/s

Shot No. 4965; velocity 201 m/s

Shot No. 4968; velocity 46.3 m/s

Shot No. 4972; velocity 64.3 m/s
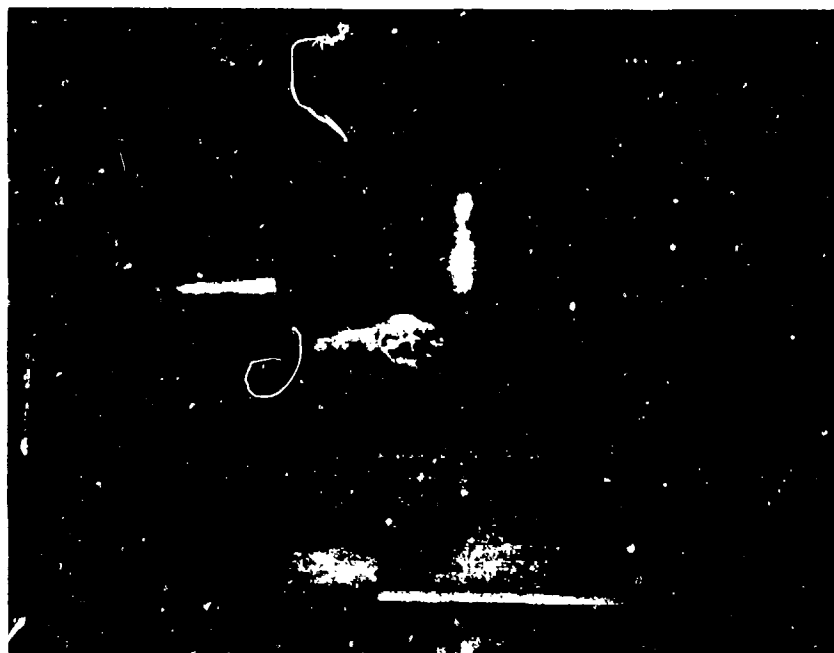
Shot No. 4973; velocity 229 m/s

Shot No. 4983; velocity 97.5 m/s
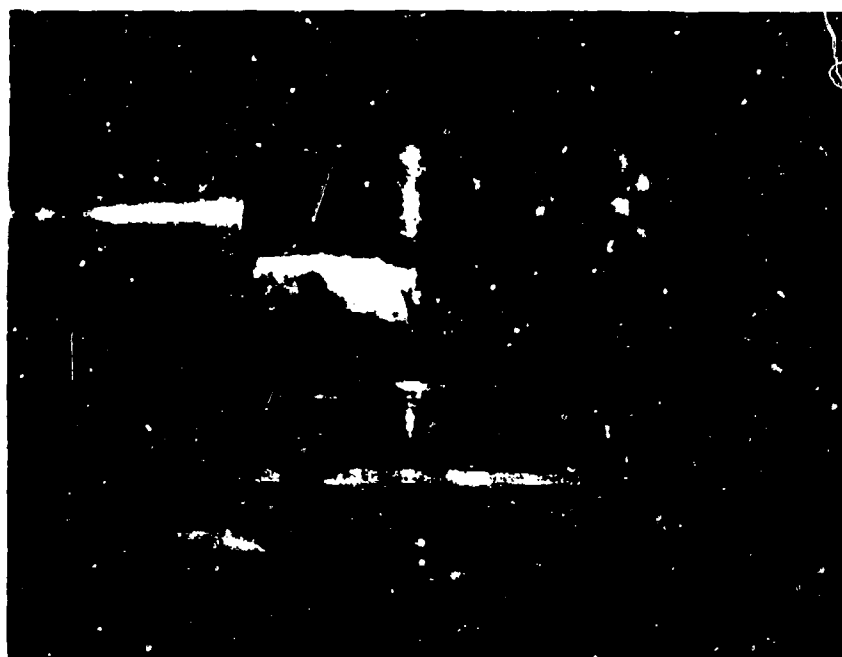
Shot No. 4984; velocity 86.0 m/s

Shot No. 4987; velocity 105 m/s

Shot No. 4988; velocity 52.7 m/s
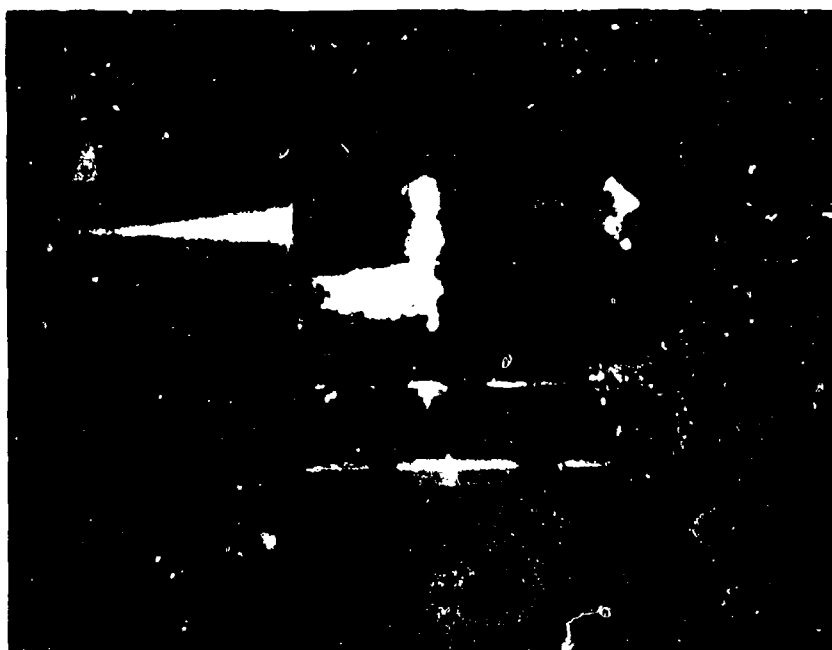
Shot No. 4990; velocity 114 m/s
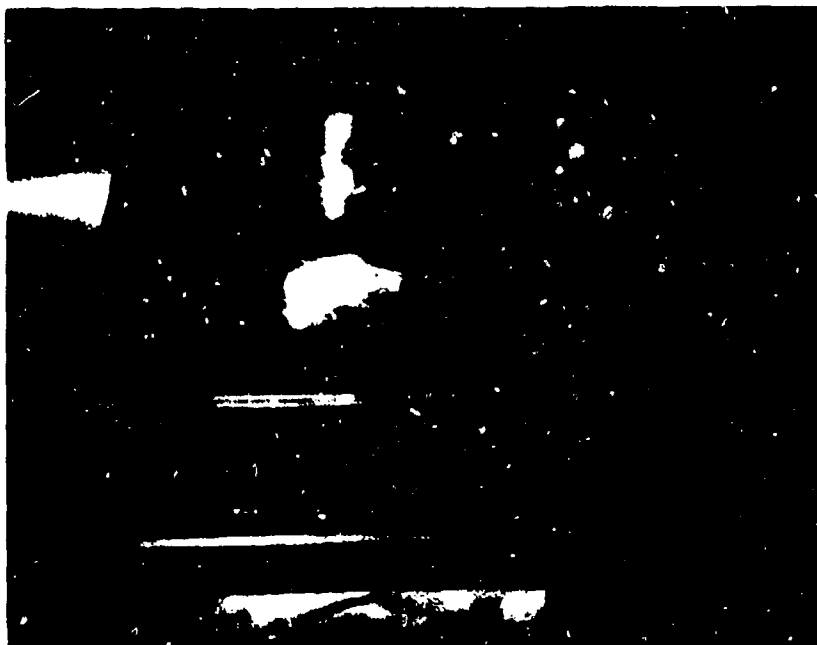
Shot No. 5002; velocity 234 m/s
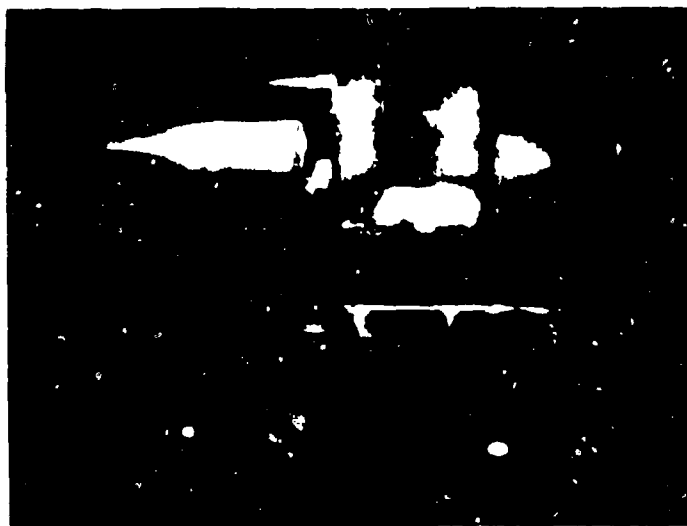
Shot No. 5190; velocity 129 m/s

APPENDIX   C

BIRD IMPACT CINE SEQUENCES
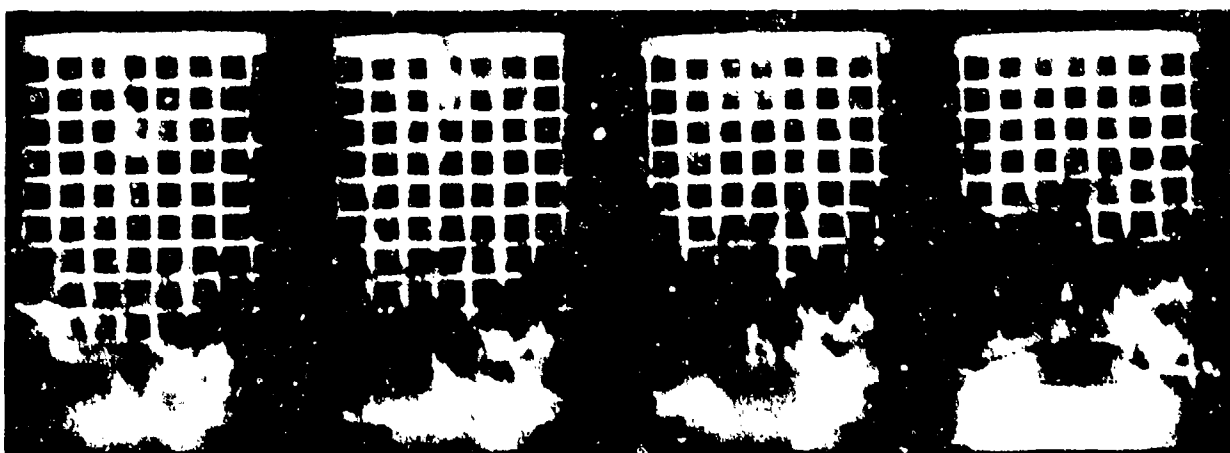
Shot No. 5133;   velocity 104 m/s,   7,460 frames/s

Shot No. 5133;   velocity 104 m/s,   7460 frames/s

Shot No. 5144;　　　　　velocity 144 m/s　　　　8, 270 frames/s

Shot No. 5144;   velocity 144 m/s,   8, 270 frames/s

Shot No. 5146; velocity 73.7 m/s, 7,720 frames/s

13   14   15   16
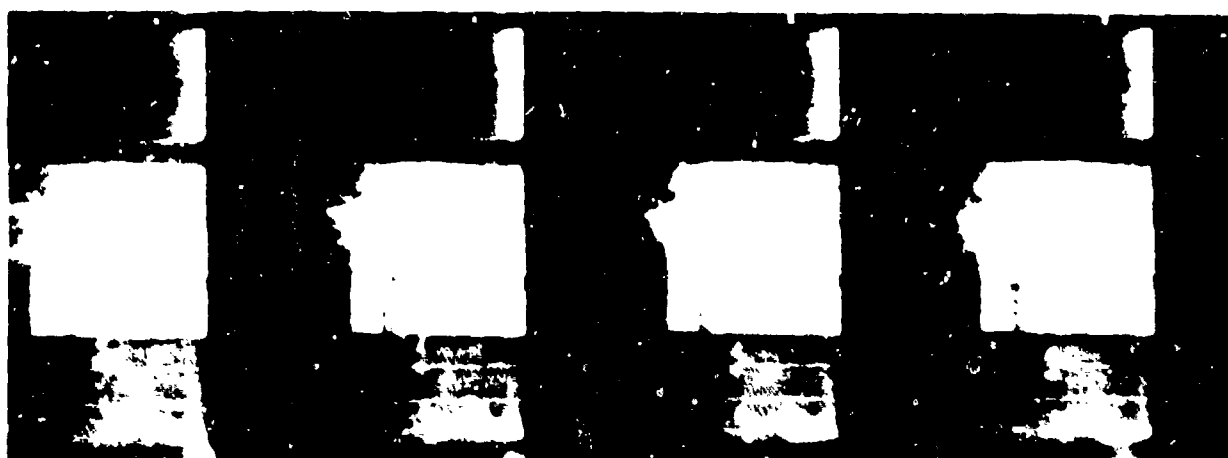
17   18   19   20

21   22   23   24

Shot No. 5146;   velocity 73.7 m/s,   7,720 frames/s

Shot No. 5149: velocity 88. 9 m/s, 7, 250 frames/s

13   14   15   16
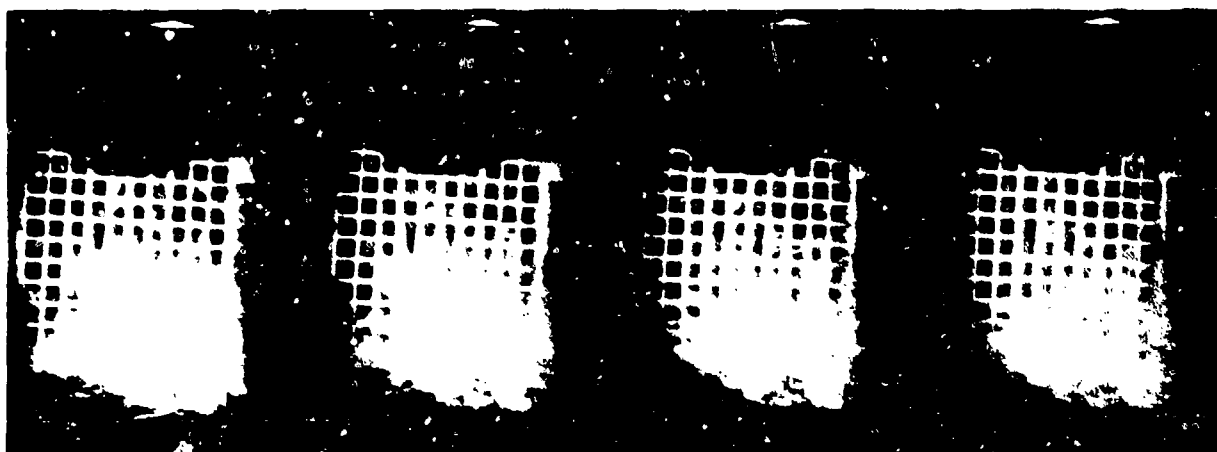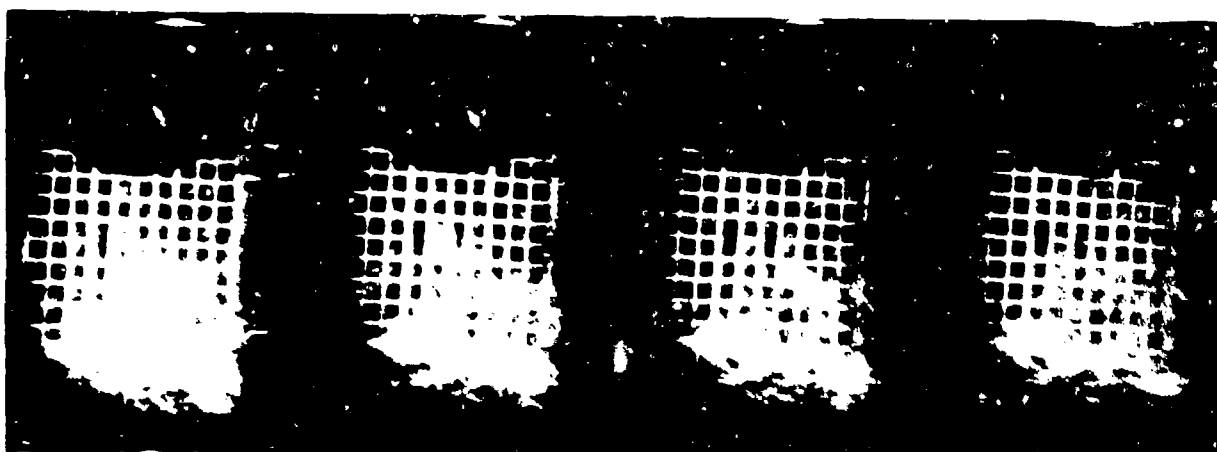
17   18   19   20

21   22   23   24

Shot No. 5149;   velocity 88 9 m/s,   7, 250 frames/s

1   2   3   4
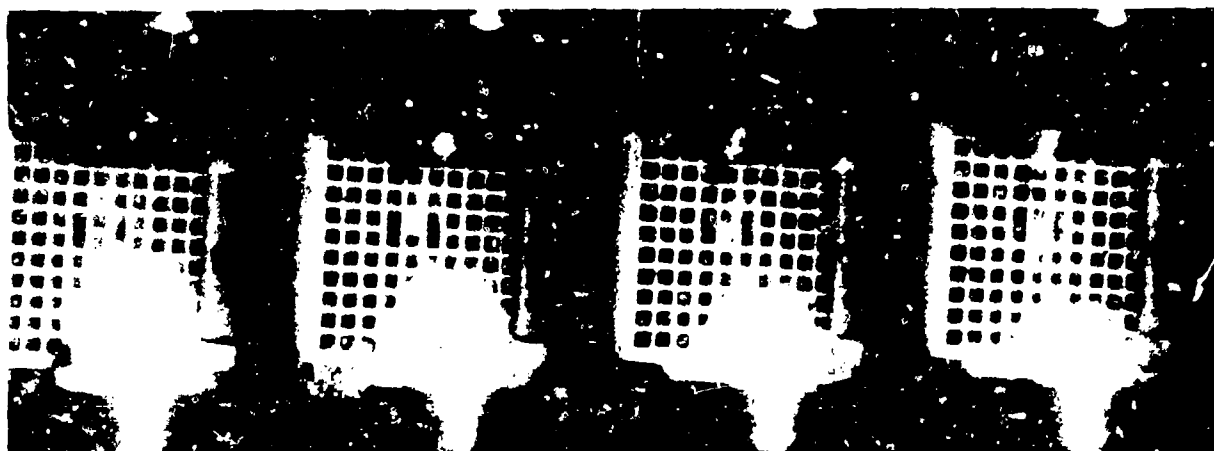
5   6   7   8
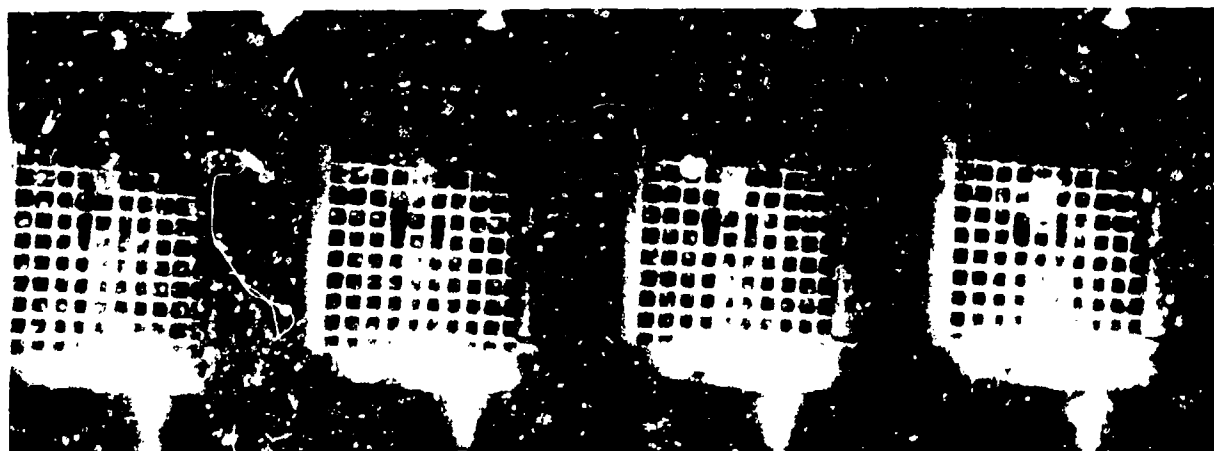
9   10   11   12

Shot No. 5150;   velocity 85. 0 m/s   7, 500 frames/s
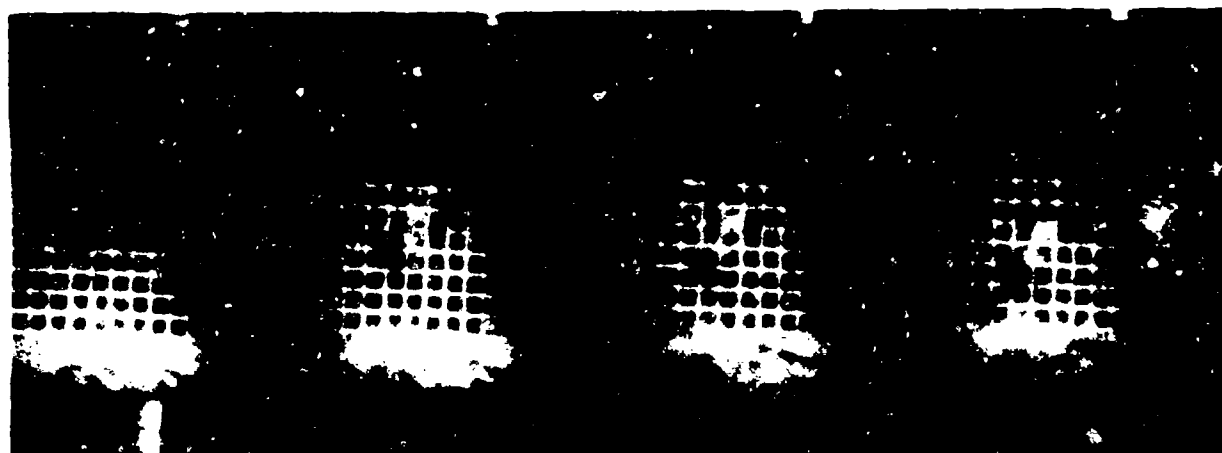
13 14 15 16
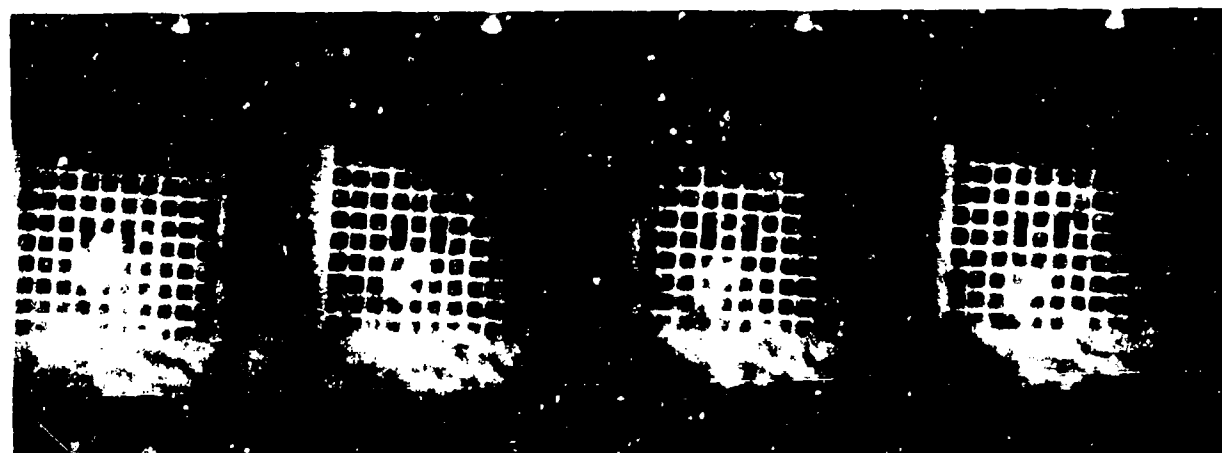
17 18 19 20
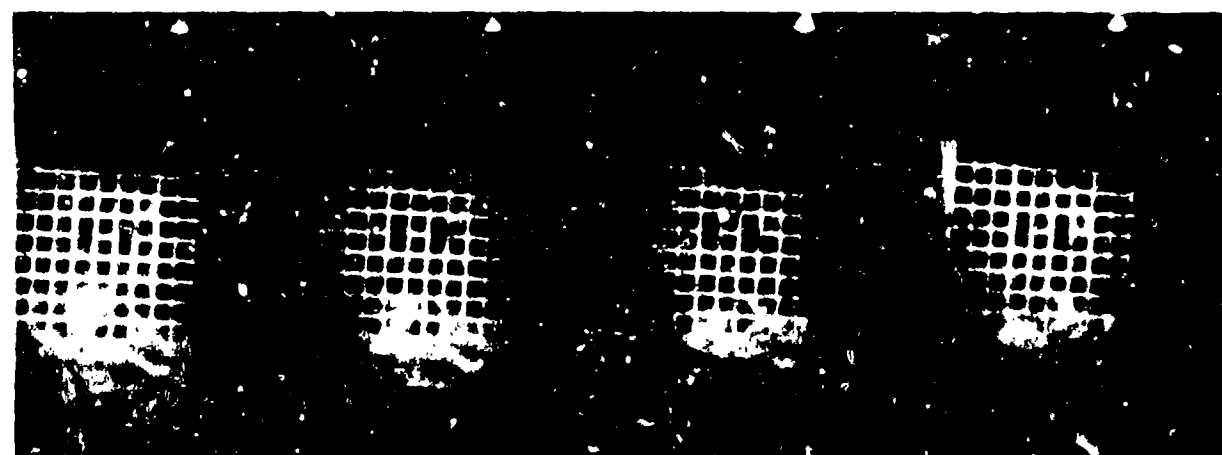
21 22 23 24

Shot No. 5150; velocity 85.0 m/s, 7,500 frames/s

APPENDIX D

INVESTIGATION OF PRESSURE TRANSDUCERS

INVESTIGATION OF PRESSURE TRANSDUCERS

1.   BACKGROUND

Air Force Materials Laboratory Impact Physics Laboratory has been studying problems involving bird impacts with aircraft transparencies for the past year. The first phase of these tests included developing techniques for launching small birds at velocities up to 1100 ft/sec without significantly damaging the bird carcasses. Specially-developed rigid targets are now being used to measure peak normal stress variations and pressure-time histories at a variety of points on the target surface. Initial investigations of commercially available piezoelectric pressure gauges suitable for making such pressure measurements indicated that their sensitivities may deviate from supplied calibration curves and that they may suffer cumulative damage from repeated vibratory accelerations received during impacts. The gauges may also be destroyed by point loading caused by impacts of sharp protrusions from launched birds (i.e., beak, legs, and bones). These potential problems are especially important since the Arnold Engineering Development Center (AEDC) is preparing to conduct a rigid plate impact experiment using up to 28 piezoelectric transducers.

2.   OBJECTIVE

The objective of the current effort is to investigate the life expectancy of candidate pressure transducers mounted in rigid plates and subjected to bird impacts. This effort also included the development of a protective covering for the transducer diaphragms which does not affect its dynamic response. A calibrating procedure was also developed which permitted dynamic transducer calibration of the gauges with or without protective coverings.

Two piezoelectric pressure transducers that are current candidates for a large bird impact experiment at AEDC were purchased by the University for testing. One transducer (PCB Model 108) has a built-in amplifier and impedance converter and the other (PCB Model 118) has the amplifier and impedance converter in the line. A table specifying their characteristics is appended to this document.

2.1 Damage Evaluation

2.1.1 Protective Coverings

Prior to the testing of candidate protective coverings the bare transducers were impacted with birds of various weights between 2-1/2 and 4-1/2 ounces launched at velocities between 200 fps to 1100 fps to provide sufficient pressure data to establish reference performance characteristics.

Three candidate materials lead, RTV rubber, and polyethylene, were selected from past ballistic experience which indicated that these materials might provide adequate transducer diaphragm protection without significantly affecting gauge response. Protective covers for the diaphragms were fabricated in the form of tablets from each candidate material. These tablets were mounted in holes in the impact plate so that one surface was flush with the plate surface and the other surface bore on the recessed transducer diaphragm. A series of bird impacts was conducted on the covered transducer and the results were compared with those from similar impacts where the transducers diaphragms were flush with the plate surface to determine the effectiveness of each material. Polyethylene proved to be superior to the other two candidates since it was the only material that provided adequate protection while transmitting the pressure pulses virtually unchanged. The lead tablet transmitted the pressure pulses satisfactorily but it swaged against the side of its housing placing a residual force on the gauge diaphragm. The RTV tablet oscillated during impact superimposing a vibratory frequency on the output pulses.

2.1.2 Lifetime Evaluation

The next phase of the transducer damage evaluation concerned the ability of the transducers to withstand repetitive impact shock loading. One type 108 transducer with its built-in amplifier and two type 118 units with separate amplifiers were mounted in a rigid plate with their diaphragms exposed. After precalibration the gauges were subjected to a series of bird impacts to determine transducer lifetimes under expected service conditions. The outputs of the transducers were recorded during each impact and were compared to one another and to previous recordings to detect faulty gauge performance. After forty-five impacts the type 108 transducer failed but the two remaining type 118's continue perform satisfactorily. From the limited number of transducers tested, our tentative conclusion is that the type 118 transducers without onboard electronic packages have a greater in-service life expectancy. We feel that it is especially important that the impacts were conducted on unprotected transducers thus providing somewhat harsher test conditions than would be expected for transducers operated with protective coverings.

2.1.3 Shock Evaluation

The magnitude of the acceleration experienced by the nominally rigid plate during impact was recorded at various locations to determine the vibratory environment experienced by the gauges. An accelerometer was positioned at different locations during subsequent bird impacts and the impulse loading on the plate recorded. The maximum vibration amplitude recorded was 80,000 g's acceleration at a 200 k Hz vibration. This vibrational load build up to peak amplitude in 150 μsec and decays to half amplitude in 500 μsec or 100 cycles. This corresponds to the fundamental frequency of the plate in the longitudinal mode. The manufacturer specifies that the gauge should be able to withstand up to a 100,000 g loading rate which is well above our maximum recorded level.

2.2 Gauge Calibration

Initial experience with the gauges indicated that they could not be calibrated using quasistatic procedures because of excessive drifts of their DC-coupled amplifiers. This problem was averted by applying 1 Hz square stress waves with rise and fall times of approximately 5 msec to the gauges and recording gauge outputs with an oscilloscope.

2.2.1 Hydraulic Calibration

To check the calibration curves provided by PCB and to provide a base against which to compare the protective covered transducer calibration data, a hydraulic test fixture was utilized to apply cyclic square waves. Peak pressures of 5000, 10,000, 15,000, and 20,000 psi were applied and transducer output was recorded. Typical results are presented in an appended figure.

2.2.2 Tests with Protective Diaphragm Coverings

The gauge to be tested was mounted in a special fixture with a polyethylene tablet against its diaphragm and a ram was brought to bear on the opposite side of the tablet. Initially, a force corresponding to a 50 psi preload was applied to the ram by an MTS machine (Materials Test Machine). The MTS was then set to provide 1 Hz cyclical square wave loads with forces corresponding to 2,000, 4,000, 6,000, 10,000, 13,500, 16,000, 18,000 and 21,000 psi and the gauge outputs were again recorded. Typical data from this is also presented in the appendix figure.

3. CONCLUSIONS

3.1 Lifetimes

The expected lifetime of the gauges appears to be connected to the location of the amplifier and impedence converter. If the package is built into the gauge, as in the 108, it is subjected to large acceleration loading which will eventually damage the effectiveness of the transducer. Therefore

transducers with the amplifier and impedance converter built in the line
as in 118 and not subjected to shock loading will have a longer life expectancy.

3.2 Protective Covering

The polyethylene protective covering did not significantly alter
the dynamic calibration performance of the PCB pressure transducers. At
lower pressures (0 to 13,500 psi) the calibration differed by less than 2%
and at higher pressures (13,500 to 21,000 psi) by less than 5% (see figure).
Noting that the operating range of the transducers will be in the 8,000 to
12,000 psi range the performance of the transducers was judged to be satis-
factory.

APPENDIX

TABLE 1
GAUGE CHARACTERISTICS

Model 118

      linearity $\pm$ 2%

      resonant frequency 300 K Hz

      rise time 2 μsec

      acceleration sensitivity psi/g .01

      press range 0 - 170 K si

      temperature range -400°F to +400°F

      vibration peak $\pm$ g 10,000

      shock -g max 20,000

Model 108

      resolution 2 psi

      resonant frequency 300 K Hz

      rise time 2 μsec

      time constant 2000 sec

      linearity $\pm$ 2%

      full scale range 100 K si

      maximum pressure 125 K si

      output impedence 100 ohms

      vibration shock 2000/20,000

      acceleration sensitivity .01 psi/g

I.C.P. TRANSDUCER DATA

PIEZOTRONICS INC.

P.O. BOX 33

BUFFALO, NEW YORK 14225

Model • *1122-P/463403*

Cal. Range *0-3g000*

S/N *223'/1216*

Input Time Constant *~.02* Sec

Rise Time *2* μSec

By *J T*

Average Sensitivity* *.587* mv psi

Natural Frequency *700* KHz

Date *3.27.74*

Linearity *< 1.0* %F.S.

Output Impedance *<100 Ohms*

*By comparison with reference Standard per ISA S 37.10

OUTPUT - MILLIVOLTS

10000

8000

6000

4000

2000

0

0   5000   10000   15000   20000   25000   30000

D-8
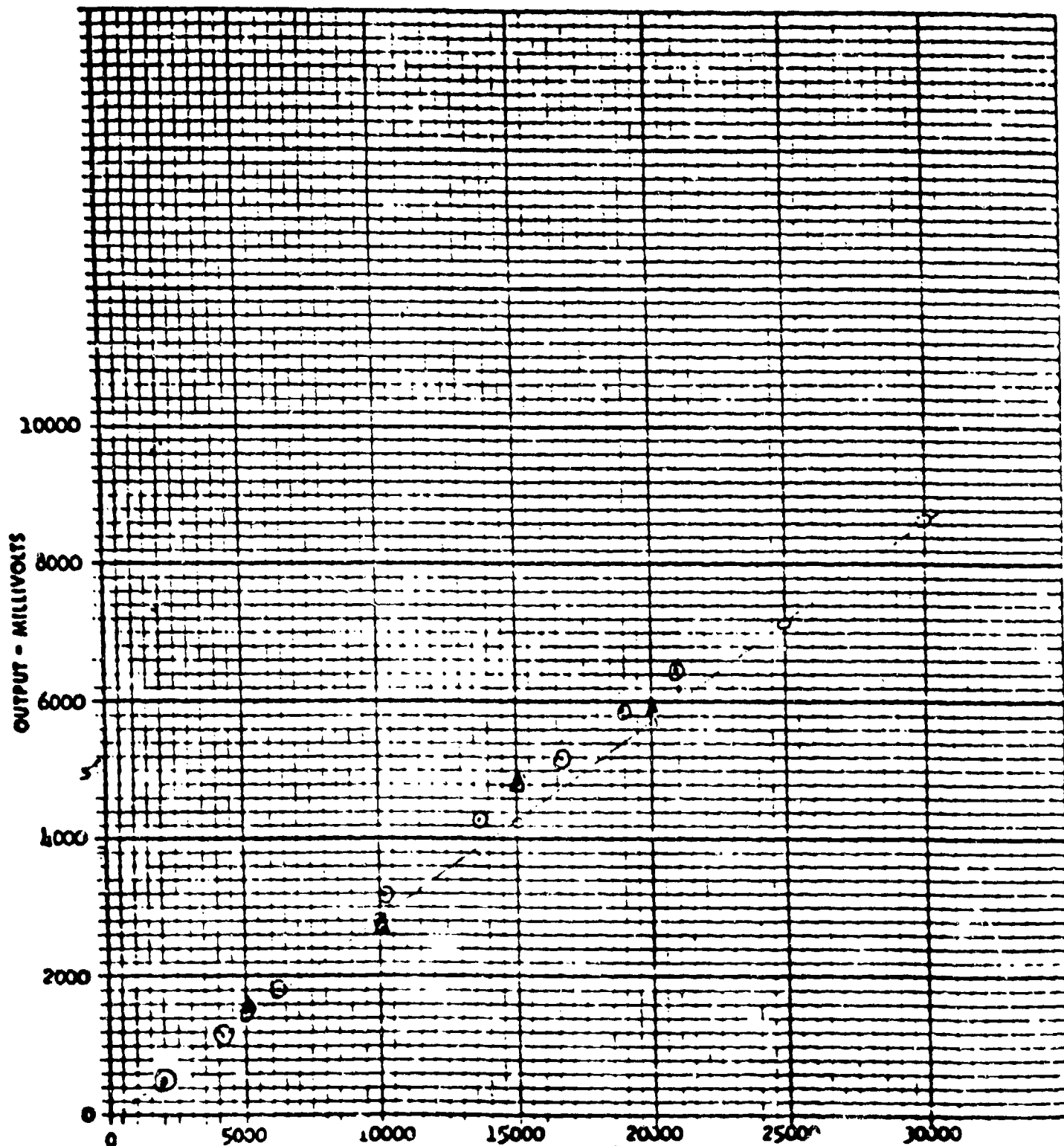
APPENDIX E

PRESSURE-TIME OSCILLOGRAPHS

This appendix contains a selected collection of oscillographs of impact pressures developed by birds impacting a flat plate.

Transducer radial position is indicated as:

A - center line of impact

B - 1.27 cm off center

C - 2.54 cm off center

D - 3.81 cm off center

SHOT NO. 4970-A
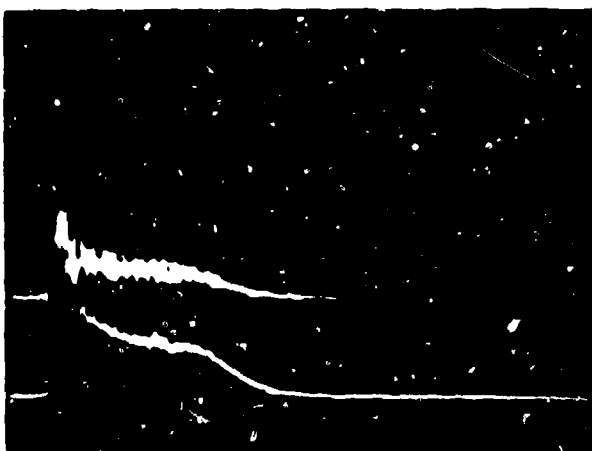
SHOT NO. 4990-B
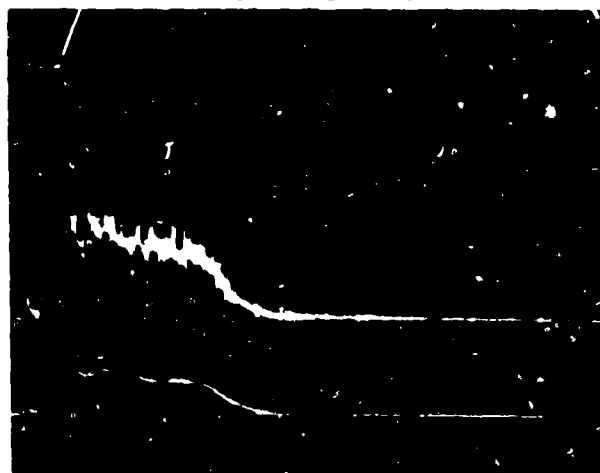
SHOT NO. 4991-B
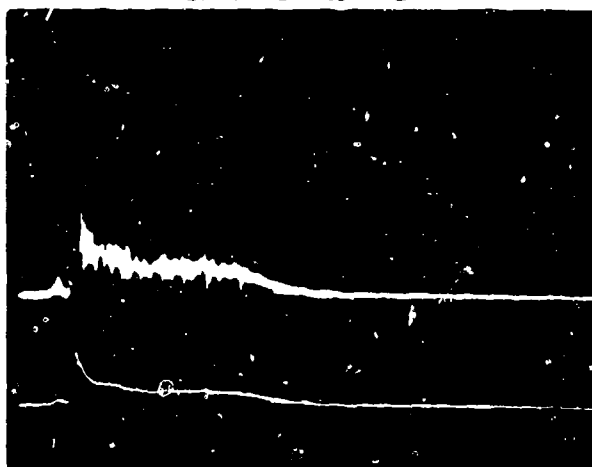
SHOT NO. 4992-B
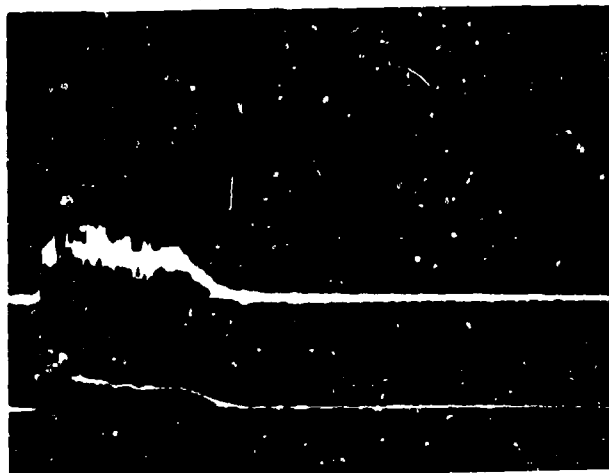
SHOT NO. 4993-B
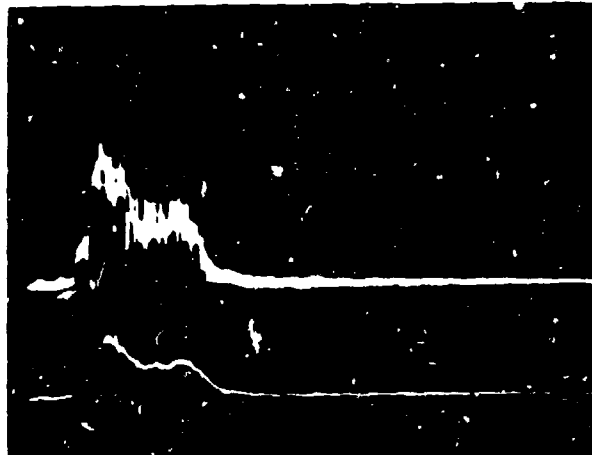
SHOT NO. 4995-B
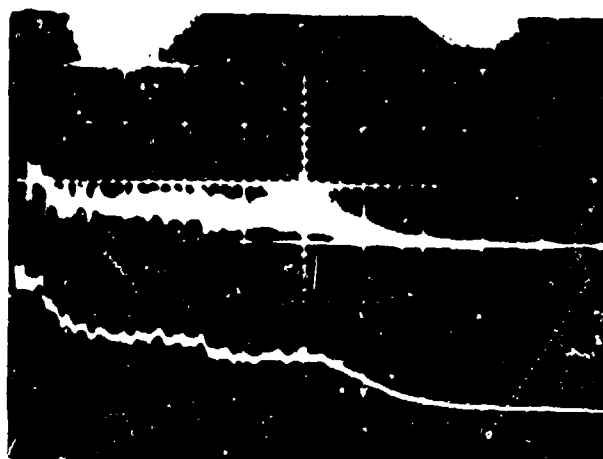
SHOT NO. 5110-A

SHOT NO. 5110-C
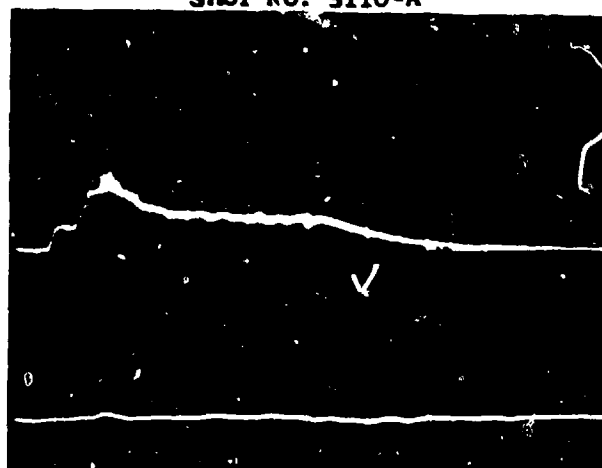
SHOT NO. 5111 $\frac{-A}{-B}$
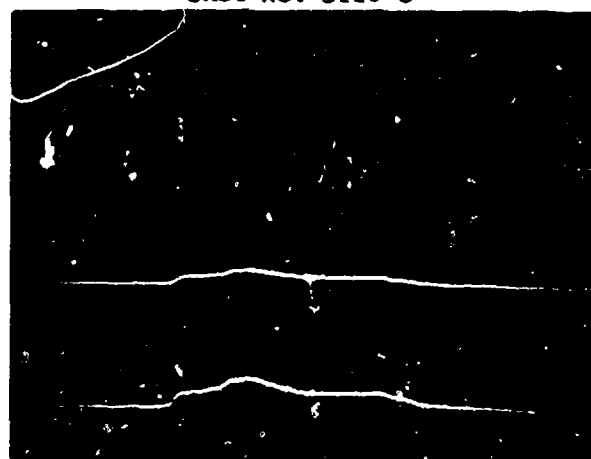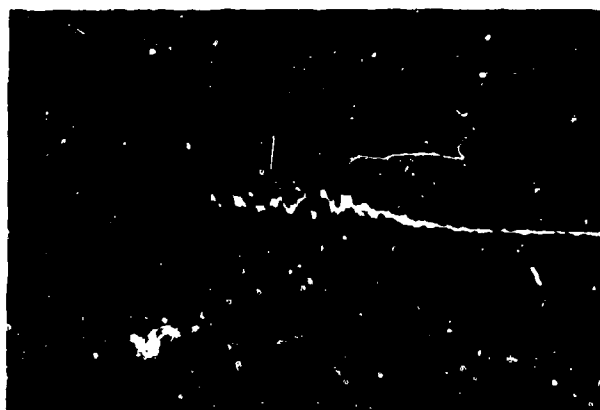
SHOT NO. 5111-C

SHOT NO. 5113-A
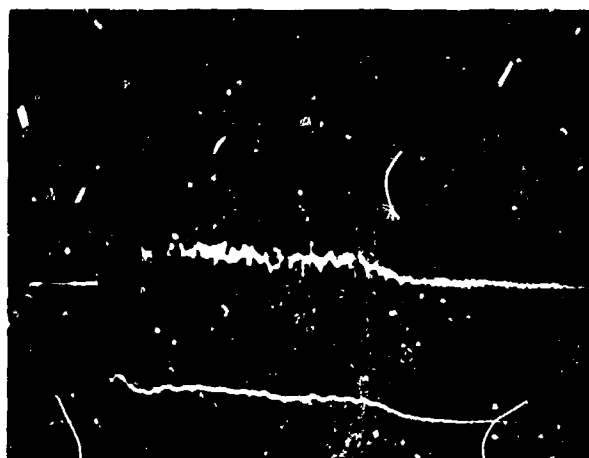
SHOT NO. 5113-C
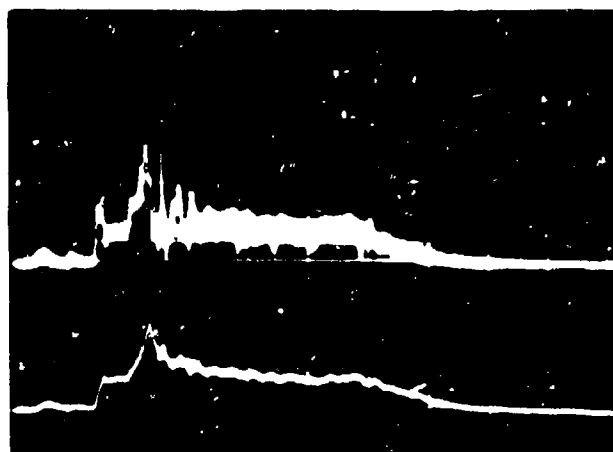
SHOT NO. 5114-A
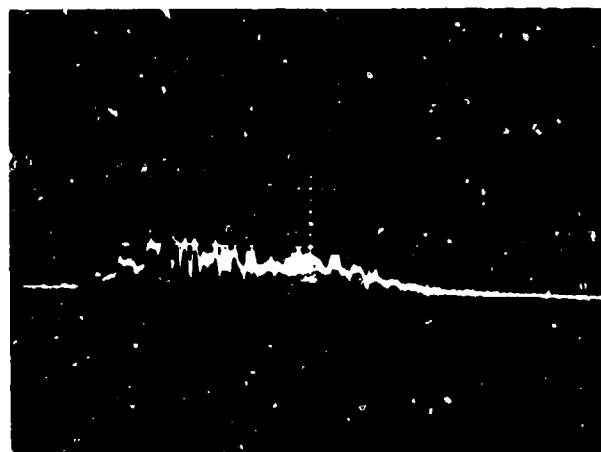
SHOT NO. 5118-A

SHOT NO. 5118-C
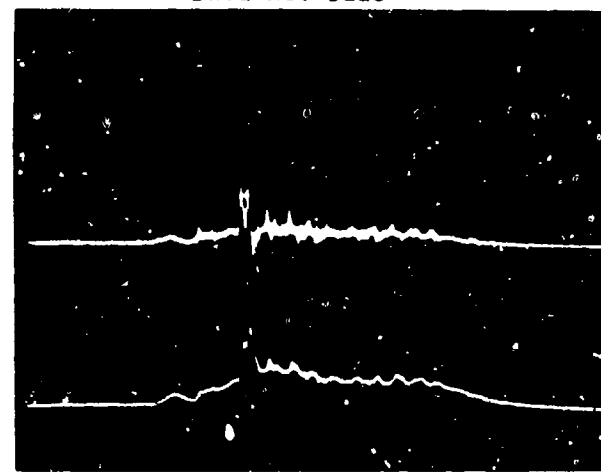
SHOT NO. 5121-A
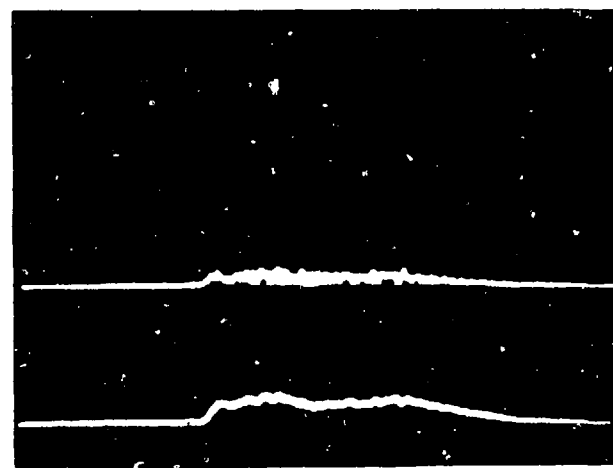
SHOT NO. 5121-C
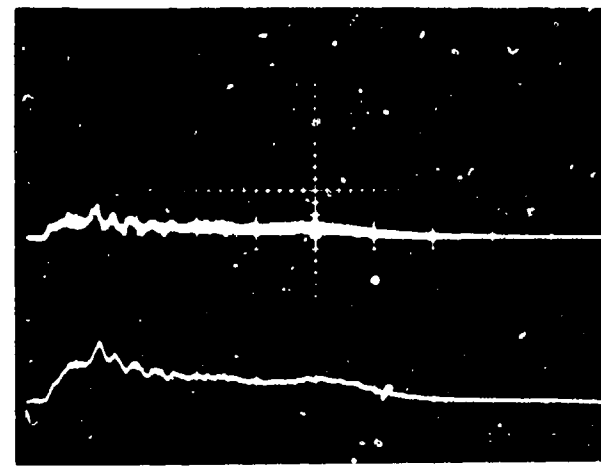
SHOT NO. 5122-A
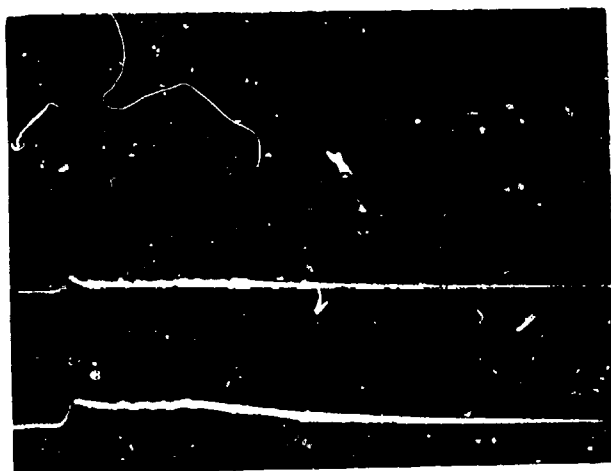
SHOT NO. 5122-C

SHOT NO. 5123-A
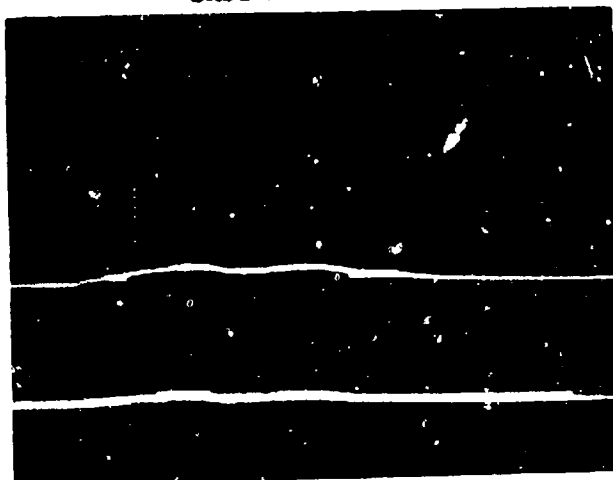
SHOT NO. 5123-C
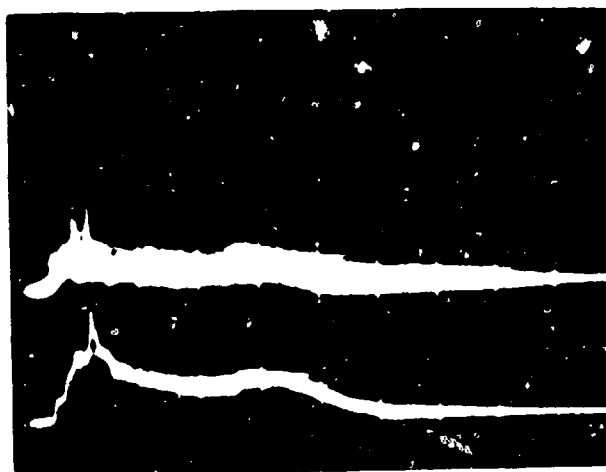
SHOT NO. 5124-A
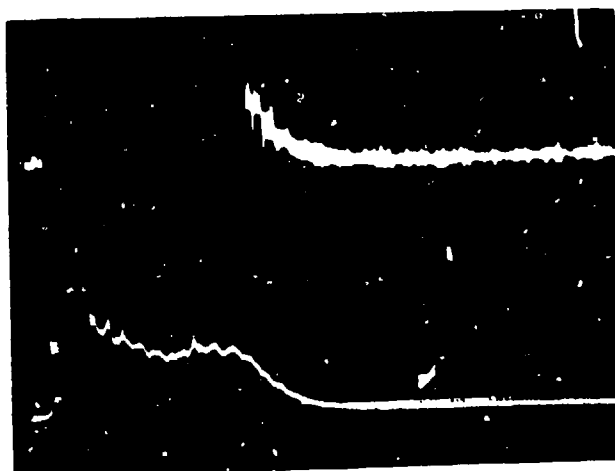
SHOT NO. 5125-A
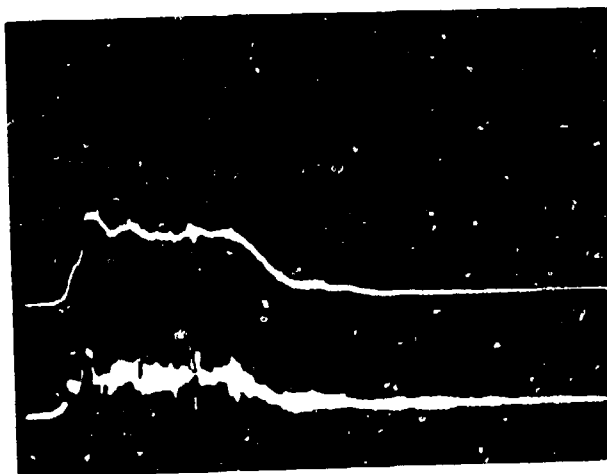
SHOT NO. 5125-C
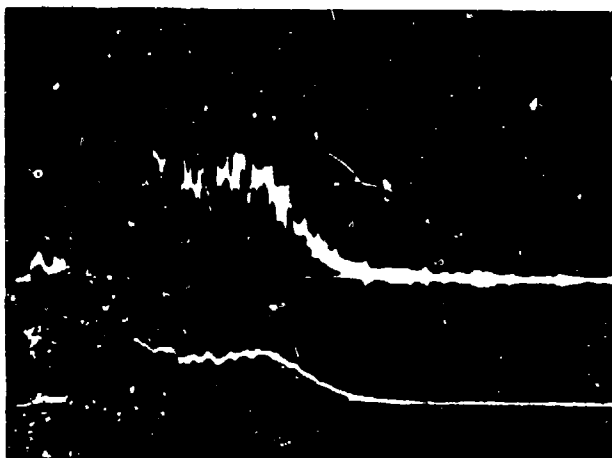
SHOT NO. 5126-A
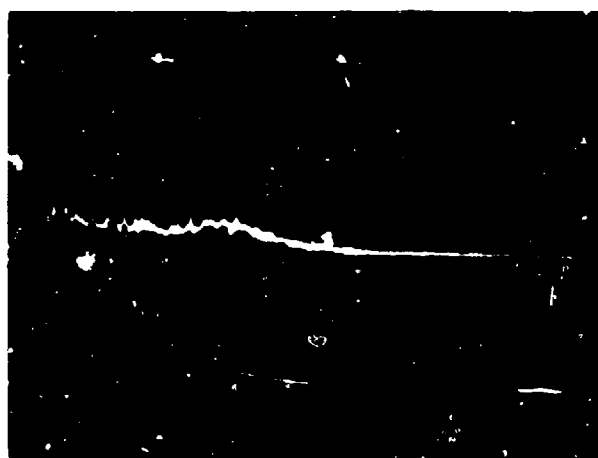
SHOT NO. 5126-B
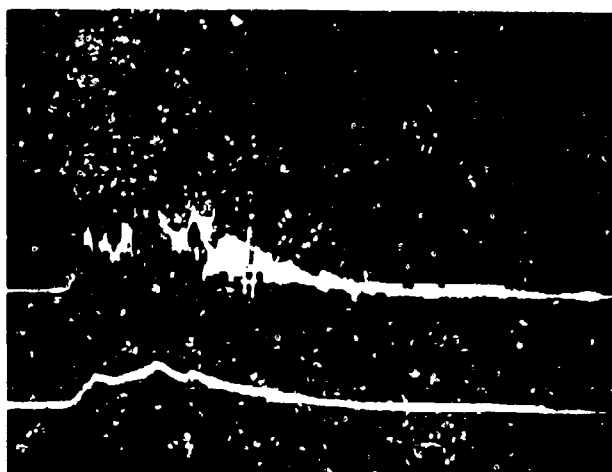
SHOT NO. 5126-C
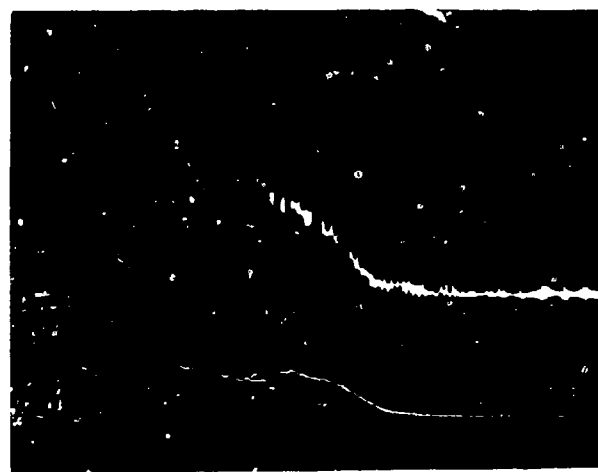
SHOT NO. 5127-A
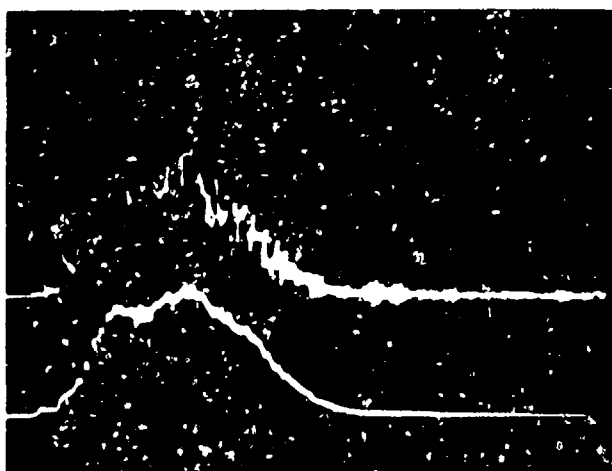
SHOT NO. 5127-C
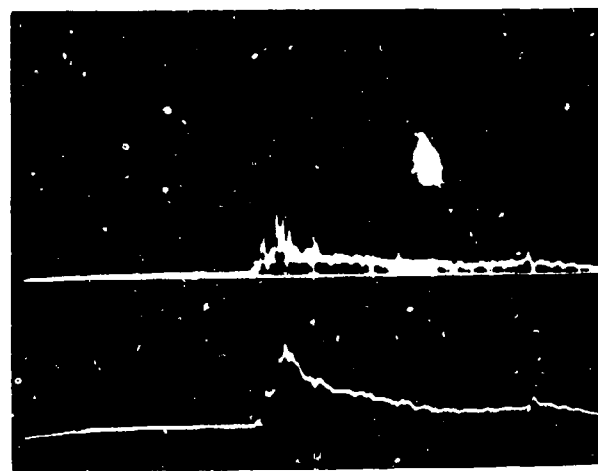
SHOT NO. 5129-A
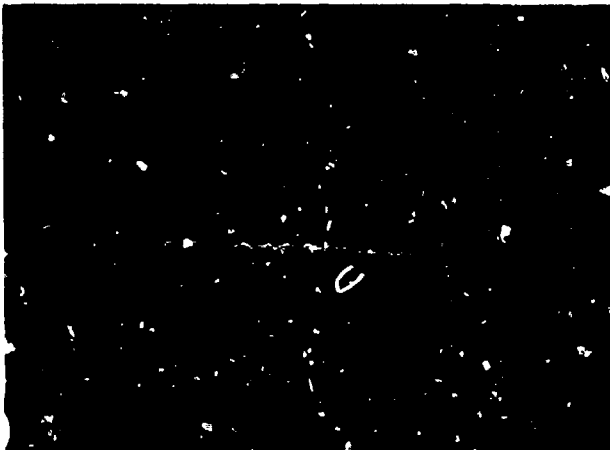
SHOT NO. 5131-A
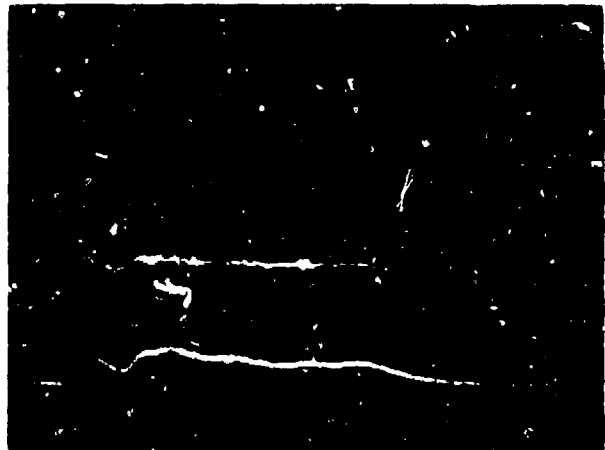
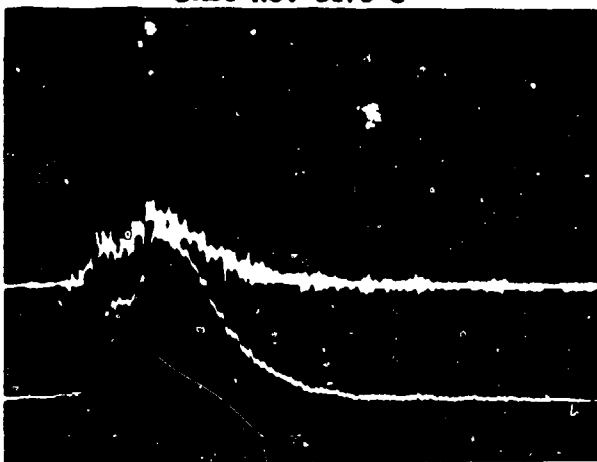SHOT NO. 5131-C
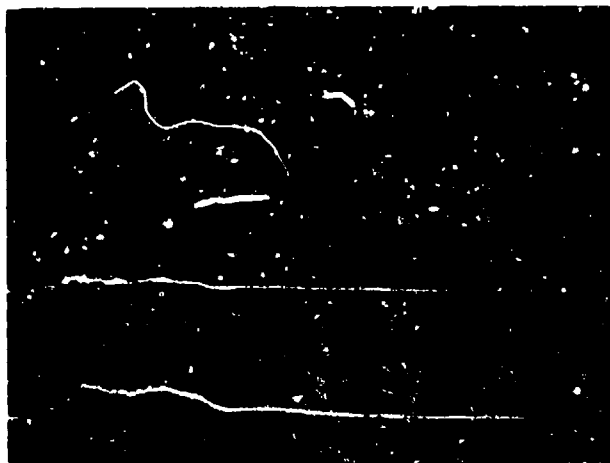
SHOT NO. 5136-C
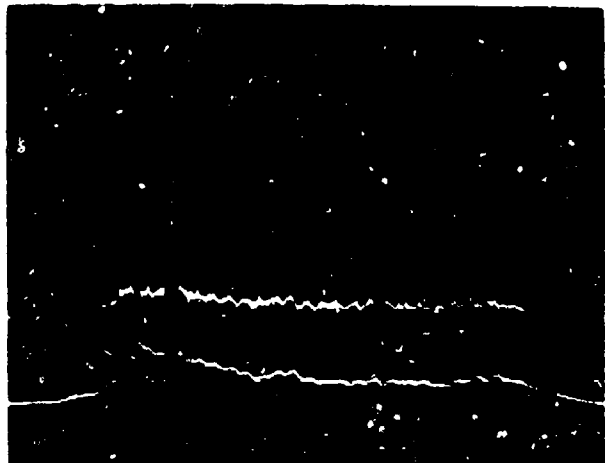
SHOT NO. 5140-A
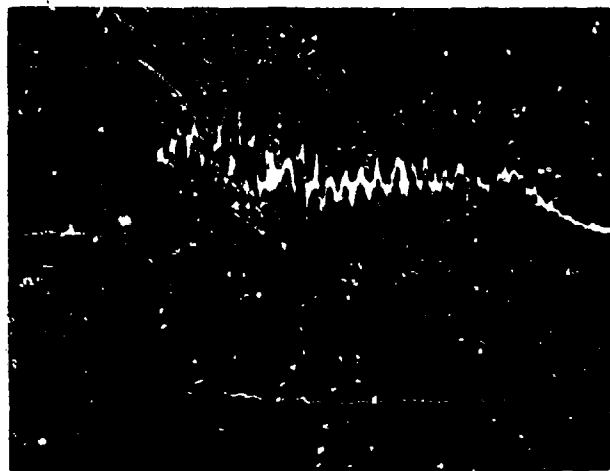
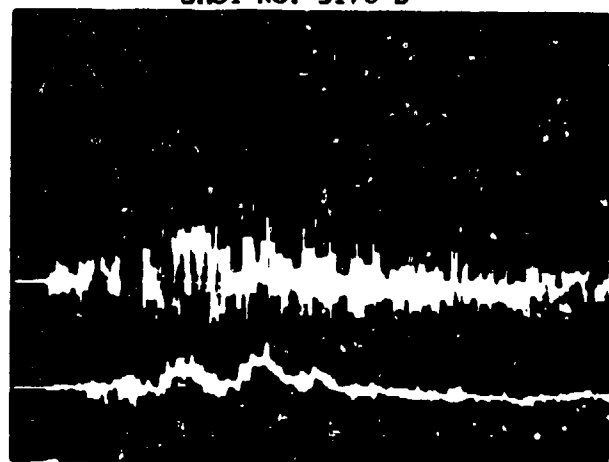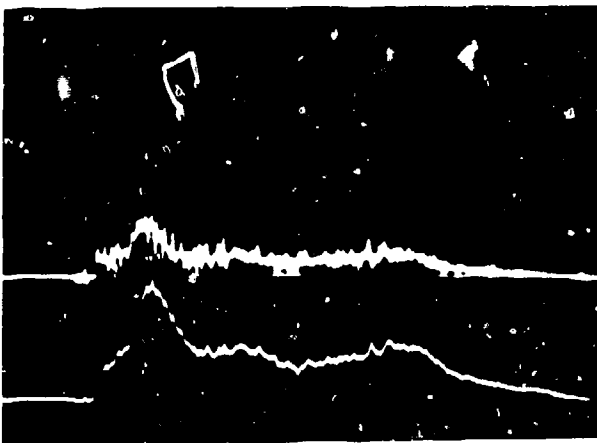SHOT NO. 5140-B
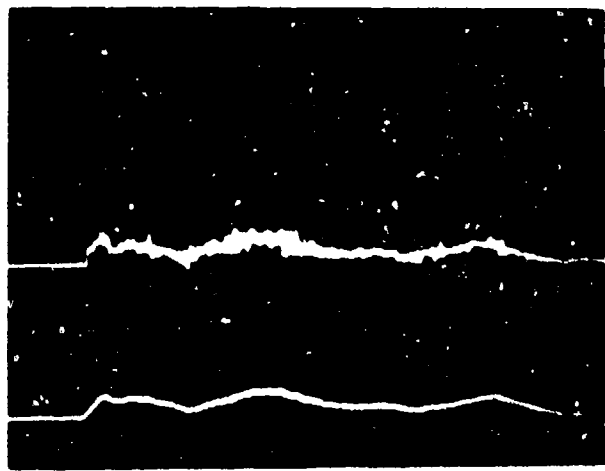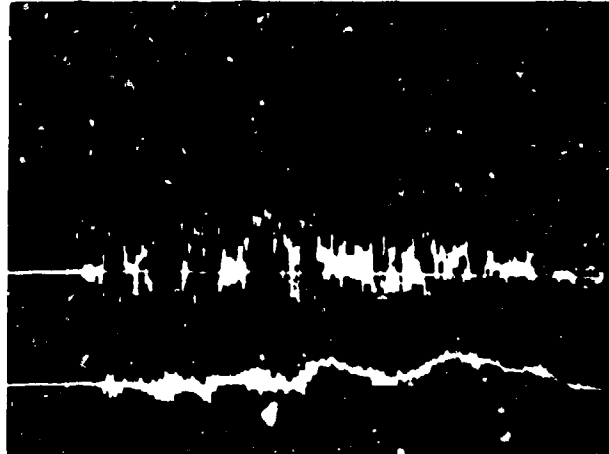
SHOT NO. 5140-C
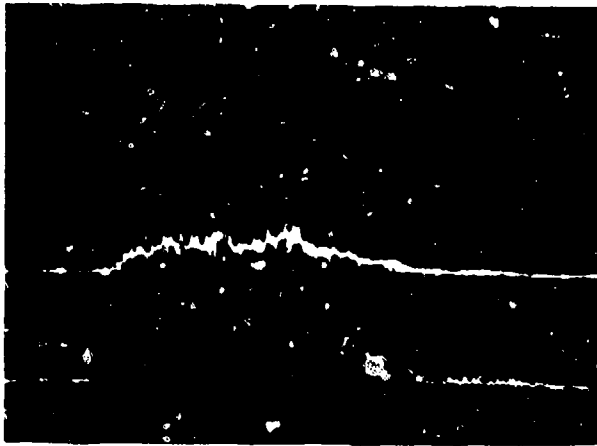
SHOT NO. 5170-C

SHOT NO. 5170-D

SHOT NO. 5172-C

SHOT NO. 5172-D

SHOT NO. 5181-C

SHOT NO. 5181-D